Table 1. Sequences of primers used for real-time reverse transcription–polymerase chain reaction with the SYBR Green detection system

Gene	Accession no.	Sense/Antisense	Sequence
Chi3l1	AA945643	Sense	5′-TCGTTAACAGGGATGACCTGTATCT-3′
		Antisense	5′-GGGTAGGACGGTGGGATTGT-3′
Slc2a3	AA901341	Sense	5′-AAGCTGGCCATTGGCAAAT-3′
		Antisense	5′-CTAGCCTCTTGTGCTCCTCCAT-3′
Slc16a6	AA859652	Sense	5′-AAAGGTGTTTCGACTGCATTCTC-3′
		Antisense	5′-CCCCATGTACCAAGCACTGTT-3′
Prlr	AW142962	Sense	5′-TGTCGCATAAGGTCCCCTCTT-3′
		Antisense	5′-GCTTGGCAATTTGTAGGGAAAG-3′
Pi4KII	BE097981	Sense	5′-CCCCTTTCTCTTTCCTTCTGGTA-3′
		Antisense	5′-ACAGCAAGTTCCAGGACAGTCA-3′
Actn1	BE119221	Sense	5′-AAGAAGGCGGTGTCTGTAAGCT-3′
		Antisense	5′-CCGTCCCTTGGCTTTGAA-3′
Pvrl3	AW525315	Sense	5′-GGCAAGACACTGGTTCTACACAAT-3′
		Antisense	5′-AAGGCCCGAAGAATGTTTTTC-3′
Rai3	BI276110	Sense	5′-GGAGCAAGTGCCAGGAATTTAT-3′
		Antisense	5′-CAGTTTTTTCCAGCCAGGAGAA-3′

Actn1, actinin α1; Chi3l1, chitinase 3-like 1; Pi4KII, phosphatidylinositol 4-kinase type 2α; Prlr, prolactin receptor; Pvrl3, poliovirus receptor-related 3; Rai3, retinoic acid induced 3; Slc2a3, solute carrier family 2 (facilitated glucose transporter) member 3; Slc16a6, solute carrier family 16 (monocarboxylic acid transporters) member 6.

adirect/ab?cmd=catNavigate2&catID=601267) (n = 5/histological preparation). For measurement of transcript levels of chitinase 3-like 1, solute carrier family 2 (facilitated glucose transporter) member 3, solute carrier family 16 (monocarboxylic acid transporters) member 6, prolactin receptor, phosphatidylinositol 4-kinase type 2α, actinin α1, *Pvrl3*, and retinoic acid induced 3, primer sets were designed using Primer Express software (Version 2.0; Applied Biosystems), and the corresponding primer sequences are shown in Table 1. Amplified transcript levels were measured with the SYBR Green detection system (n = 5/histological preparation). For quantification of expression data, a standard curve method was applied using the first-round antisense RNA prepared for microarray analysis from NTF as a standard sample. Expression values were normalized to two housekeeping genes, glyceraldehyde 3-phosphate dehydrogenase and hypoxanthine-guanine phosphoribosyltransferase, as described previously.[14]

Immunohistochemistry. The cranial halves of the bilateral thyroids of SDM-promoted animals were subjected to fixation in 10% phosphate-buffered formalin (pH 7.4) solution for 2 days at room temperature, and prepared for histopathological examination. In untreated controls and DHPN-alone cases, whole thyroid tissue was fixed in buffered formalin and prepared similarly.

Immunohistochemistry was carried out with antibodies against ceruloplasmin (clone 8, mouse IgG_1, 1:50; BD Transduction Laboratories, San Jose, CA, USA), Ccnb1 (clone V152, mouse IgG_1, 1:100; Thermo Fisher Scientific Inc., Fremont, CA, USA), Cdc2 (clone A17, mouse IgG_{2a}, 1:200; GeneTex, San Antonio, TX, USA), thyroglobulin (clone SPM221, mouse IgG_1, 1:250; Spring Bioscience, Fremont, CA, USA), Pvrl3 (goat IgG, 1:100; R&D Systems, Minneapolis, MN, USA), and Id3 (rabbit IgG, 1:100; ProteinTech Group, Chicago, IL, USA). For confirmation of positive immunoreactivity of antigens examined, normal rat tissues, such as the liver for ceruloplasmin,[19] duodenal mucosa for Ccnb1 and Cdc2, and thyroid for thyroglobulin,[20] Pvrl3, and Id3, were used. For each antigen, subcellular or extracellular localization was examined and compared to the cases previously reported.[21–26] Optimal conditions for antigen retrieval were also determined using positive control tissues. For antigen retrieval, deparaffinized sections were heated in 10 mM citrate buffer (pH 6.0) by autoclaving for 10 min before incubation with the Ccnb1 and Pvrl3 antibodies, or for 20 min before incubation for ceruloplasmin, Cdc2, and Id3. No antigen retrieval treatment was carried out for thyroglobulin. Immunodetection was carried out utilizing a Vectastain Elite ABC kit (Vector Laboratories, Burlingame, CA, USA), with 3,3′-diaminobenzidine/H_2O_2 as the chromogen, as described previously.[15] As negative controls for immunoreactivity, normal serum from mouse, goat, or rabbit was applied to rat positive control tissues with appropriate dilutions instead of the primary antibodies. Sections were counterstained with hematoxylin.

Analysis of immunoreactivity. For all antigens examined in the present study, immunoreactivity was essentially unaltered in the thyroids between the groups of untreated controls and DHPN alone, and these animals did not develop any proliferative lesion. Therefore, immunoreactivity scores in these groups were counted together and represented as 'normal follicular cells' with three randomly selected microscopic areas at 200-fold magnification in one animal. Animals examined for 'normal follicular cells' were nine untreated controls and five treated with DHPN. In the SDM-promoted cases, immunoreactivity scores were counted in the histological categories of NTF, FFCH + Ad, and Ca. With regard to NTF, three randomly selected microscopic areas at 200-fold magnification were subjected to evaluation for each animal. With Ca, both capsular invasive and parenchymal Ca were analyzed. Immunoreactivity in each histological type was not essentially different between the cases after 10 and 15 weeks of promotion, and therefore immunolocalization scores were counted together for these two time points. The numbers of animals examined for proliferative lesions and surrounding NTF were 10 and 11 after 10 and 15 weeks of promotion, respectively.

For ceruloplasmin, Ccnb1, Cdc2, Id3, and thyroglobulin, immunolocalization was scored as 0 (negative), 1 (slight), 2 (moderate), or 3 (prominent). In the case of Pvrl3, scores were 0 (negative), 1 (partially positive), or 2 (positive). Detailed criteria for the immunoreactivity for each molecule given in Table 2 were determined after due consultation of two independent pathologists. Immunoreactivity score in each lesion was double-checked by one pathologist and then cross-checked by another pathologist.

Data analysis. Expression values from the real-time RT-PCR were analyzed by Student's or Welch's t-test following a test for equal variance. Scores for immunoreactivity were assessed with Mann–Whitney's U-test, comparing NTF and normal follicles, FFCH + Ad or Ca. For the microarray data, the statistical analysis was carried out with GeneSpring software, and the significance

Table 2. Scoring criteria for immunohistochemical localization

Molecule	Immunolocalization for evaluation	Score of immunoreactivity			
		0	1	2	3
Ceruloplasmin	Luminal cellular surface	—	Weakly positive, a few follicles	Strongly positive, focal follicular populations	Strongly positive, majority of follicles
Ccnb1	Cytoplasm	—	Weakly positive, a few cells	Weakly positive, majority of cells	Strongly positive, majority of cells
Cdc2	Cytoplasm and nucleus	—	1–10 cells/400× field	10–30 cells/400× field	> 30 cells/400× field
Thyroglobulin	Cytoplasm	—	< 20% cells	20–70% cells	> 70% cells
Pvrl3	Intercellular membrane	—	Focally positive	Entirely positive	Not applied
Id3	Nucleus	—	Weakly positive, a few cells	Weakly positive, majority of cells	Strongly positive, majority of cells

Ccnb1, Cyclin B1; Cdc2, cell division cycle 2; Id3, inhibitor of DNA binding 3; Pvrl3, poliovirus receptor-related 3.

of gene expression changes was analyzed by Student's *t*-test or ANOVA between NTF and normal follicles, FFCH + Ad or Ca.

Results

Microarray analysis. As genes showing altered expression specifically in FFCH + Ad, 40 examples were upregulated and 20 examples were downregulated, as compared with surrounding NTF (Table 3; Supporting Tables S1, S2). In the Ca cases, the numbers of genes specifically upregulated and downregulated were 69 and 142, respectively. Representative genes with known annotations associated with carcinogenesis are listed in Table 3. Interestingly, a cluster of cell cycle-related genes were found to be upregulated specifically in FFCH + Ad, such as ubiquitin-like with PHD and RING finger domains 1, kinesin family member 23, cyclin A2, M-phase phosphoprotein, topoisomerase (DNA) 2α, Cdc2 homolog A, Ccnb1, and cyclin-dependent kinase inhibitor 3. Extracellular matrix proteins, laminin γ2, and fibronectin 1 also showed upregulation in FFCH + Ad. No particular functional cluster was observed for downregulated genes in FFCH + Ad cases. Among the upregulated genes in Ca, examples with functions in transport (ceruloplasmin) and biosynthesis (thyroglobulin) were found, whereas downregulated genes typically involved functions in tumor suppression, such as: decorin, reversion-inducing-cysteine-rich protein with kazal motifs, creatine kinase mitochondrial 1 ubiquitous, retinoblastoma 1, lysyl oxidase, and NAD(P)H dehydrogenase quinine 1. Transcript levels for genes encoding signal transduction molecules and transcription factors were also downregulated in Ca. All isoforms of Id were found to be reduced.

With regard to genes showing altered expression in common in FFCH + Ad and Ca, totals of 93 and 53 were upregulated and downregulated, respectively (Table 4; Supporting Table S3). Upregulated genes included examples linked to transport, cell proliferation, and tumor progression. In particular, multiple gene probes in the array showed increased signals for ceruloplasmin and solute carrier family 16 (monocarboxylic acid transporters) member 6. Among the genes that showed downregulation, no particular functional clusters were apparent. Two gene probes for *Pvrl3* in the array demonstrated downregulation. Real-time RT-PCR for validation of microarray data was carried out for 11 genes showing commonly altered expression with FFCH + Ad and Ca, eight upregulated and three downregulated, the results being summarized in Table 5. In both FFCH + Ad and Ca, many expression changes were similar with the two analysis systems, despite a lower magnitude of alteration observed with PCR data for the upregulated genes when the values were normalized to hypoxanthine-guanine phosphoribosyltransferase levels. With regard to downregulated genes, variability of PCR data in the NTF after normalization to the hypoxanthine-guanine phosphoribosyltransferase level was slightly higher than with glyceraldehyde 3-phosphate dehydrogenase (data not shown), and therefore statistical significance was not attained for FFCH + Ad.

Immunolocalization in the thyroid in relation to proliferative lesions. Ceruloplasmin was immunolocalized mainly at the luminal surfaces of cell membranes of follicular cells, almost specific to the proliferative lesions (Fig. 2a). Diffuse or granular immunoreactivity was also observed in the follicular lumina of lesions showing cell surface immunoreactivity. In parallel with the upregulation of transcript levels both in microarray and real-time RT-PCR analyses, immunolocalization of ceruloplasmin was specifically observed in all types of proliferative lesions, with statistical significance in the scores as compared with NTF. Although the intensity was weak, increased cytoplasmic staining was also observed in some Ca.

Ccnb1 was immunolocalized in the cytoplasm of follicular cells with fine granular immunoreactivity (Fig. 2b). In the normal follicles and NTF, weak and sparse immunolocalization was typical. In the proliferative lesions, the expression pattern of this molecule was either sparse or diffuse, and staining was weak with the former and either weak or strong with the latter. In parallel with upregulation of transcript levels in microarray analysis, a significant increase in the immunolocalization scores was observed in FFCH + Ad as compared with surrounding NTF. Although statistically significant elevation was still evident, immunoreactivity was less intense in Ca than in FFCH + Ad.

Immunoreactivity of Cdc2 was strong and localized both to the cytoplasm and nucleus of tumor follicular cells (Fig. 2c). In the normal follicles and NTF, immunoreactive cells were rather few. Although microarray data showed upregulation only in FFCH + Ad, both FFCH + Ad and Ca showed statistically significant increases in the immunolocalization scores as compared with NTF. Ca demonstrated the highest scores.

Thyroglobulin showed strong and granular immunolocalization in the cytoplasm of normal and non-tumor follicular cells as well as diffuse immunoreactivity in the follicular lumina (Fig. 2d). Although microarray data showed upregulation of the transcript levels in Ca, follicular proliferative lesions showed large variability in the immunoreactivity, and Ca showed a significant decrease in immunolocalization scores as compared with NTF.

Pvrl3 showed intercellular membrane immunolocalization in the normal and non-tumor follicular cells (Fig. 2e). With both FFCH + Ad and Ca, in parallel with the downregulation of the transcript levels common to microarray and real-time RT-PCR analyses, statistically significant decreased immunolocalization scores were observed as compared with NTF. However, the magnitude of the decrease in FFCH + Ad was stronger than in the Ca case, contrasting with the transcript data.

Inhibitor of DNA binding 3 showed nuclear immunoexpression in normal and non-tumor follicular cells (Fig. 2f). Although microarray analysis showed statistically significant downregulation of transcript levels only in Ca, statistically significant decreases

doi: 10.1111/j.1349-7006.2009.01094.x

Table 3. List of representative genes with known functional annotations associated with carcinogenesis showing altered expression specifically in thyroid proliferative lesions of each category induced in rats using a two-stage thyroid carcinogenesis model (≥2-fold, ≤0.5-fold)†

Gene function	Accession no.	Gene title	Symbol	FFCH + Ad	Ca
FFCH + Ad					
Upregulated genes (of 40 genes in total)					
Cell cycle	BE098732	Ubiquitin-like, containing PHD and RING finger domains, 1	Uhrf1	2.43	1.81
Cell cycle	BE113443	Kinesin family member 23‡	Kif23	2.20	1.09
Cell cycle	AA998516	Cyclin A2	Ccna2	2.13	1.29
Cell cycle	BM385445	Topoisomerase (DNA) 2α	Top2a	2.12	1.37
Cell cycle	BE110723	M-phase phosphoprotein 1‡	Mphosph1	2.09	1.35
Cell cycle	NM_019296	Cell division cycle 2 homolog A (*S. pombe*)	Cdc2a	2.04	1.45
Cell cycle	X64589	Cyclin B1	Ccnb1	2.01	1.40
Cell cycle	BE113362	Cyclin-dependent kinase inhibitor 3‡	Cdkn3	1.97	1.18
Metastasis	BM385282	Laminin, γ2	Lamc2	2.90	1.25
Metastasis	AA893484	Fibronectin 1	Fn1	2.16	1.40
Downregulated genes (of 20 genes in total)					
Metastasis	BE117767	Immunoglobulin superfamily, member 4A‡	Igsf4a	0.46	0.73
Cell differentiation	BG666709	N-myc downstream regulated 4	Ndr4	0.50	0.51
Ca					
Upregulated genes (of 69 genes in total)					
Biosynthesis	AI500952	Thyroglobulin	Tg	1.72	2.65
Transport	AF202115	Ceruloplasmin	Cp	1.99	2.45
Transport	BE106526	Solute carrier family 6 (neurotransmitter transporter, GABA), member 11	Slc6a11	1.44	1.98
Cell growth	M57668	Prolactin receptor	Prlr	1.78	2.42
Cell cycle	NM_133578	Dual specificity phosphatase 5	Dusp5	1.74	2.02
Proto-oncogene	NM_012874	v-ros UR2 sarcoma virus oncogene homolog 1 (avian)	Ros1	1.59	1.98
Metastatic regulator	AI175048	Sine oculis homeobox homolog 1 (*Drosophila*)	Six1	1.62	1.96
Glycolysis	BI294137	Hexokinase 2	Hk2	1.20	1.87
Downregulated genes (of 142 genes in total)					
Tumor suppressor	BM390253	Decorin	Dcn	0.76	0.27
Tumor suppressor	AW523759	Reversion-inducing-cysteine-rich protein with kazal motifs‡	Reck	0.65	0.32
Tumor suppressor	BI301453	Creatine kinase, mitochondrial 1, ubiquitous	Ckmt1	0.49	0.35
Tumor suppressor	AI178012	Retinoblastoma 1	Rb1	0.75	0.38
Tumor suppressor	NM_017061 (BI304009)	Lysyl oxidase	Lox	0.81 (0.91)	0.39 (0.49)
Tumor suppressor	J02679	NAD(P)H dehydrogenase, quinone 1	Nqo1	0.57	0.42
Signal transduction	U78517	cAMP-regulated guanine nucleotide exchange factor II	Rapgef4	0.65	0.32
Signal transduction	AA945708	Calcitonin receptor-like	Calcrl	0.59	0.34
Signal transduction	BI295477	G protein-coupled receptor 116	Gpr116	0.61	0.45
Signal transduction	NM_030829	G protein-coupled receptor kinase 5	Gprk5	0.66	0.48
Cell adhesion	NM_031050	Lumican	Lum	0.99	0.33
Transcription	AF000942	Inhibitor of DNA binding 3, dominant negative helix-loop-helix protein	Id3	0.57	0.33
Transcription	BE116009	Inhibitor of DNA binding 4	Idb4	0.56	0.40
Transcription	NM_053713	Kruppel-like factor 4 (gut)	Klf4	0.67	0.40
Transcription	M86708	Inhibitor of DNA binding 1, helix-loop-helix protein (splice variation)	Id1	0.64	0.44
Transcription	AI008792	Inhibitor of DNA binding 2, dominant negative helix-loop-helix protein	Id2	0.68	0.48
Metastasis suppressor	AI578087 (AW435343)	transmembrane 4 superfamily member 1‡	Tm4sf1	0.64 (0.74)	0.36 (0.48)
Apoptosis	AA892770	Glutamate-cysteine ligase, catalytic subunit	Gclc	0.61	0.41
Tumor metastasis	NM_133526	Transmembrane 4 superfamily member 3	Tm4sf3	0.70	0.41

Ad, adenoma; Ca, carcinoma; FFCH, focal follicular cell hyperplasias.
†Proliferative lesions were divided into two categories, i.e. FFCH + Ad and Ca.
‡Predicted gene identity.

in the nuclear immunolocalization scores were also observed in FFCH + Ad.

Discussion

With the present microdissected lesion-specific gene expression profiling, alteration was found for 60 genes specifically in FFCH + Ad, 211 genes specifically in Ca, and 146 genes in common in both, as compared with surrounding NTF. On selection of these with known annotations associated with carcinogenesis, we found upregulation of cell cycle-related genes specifically in the early proliferative lesions, represented by FFCH and Ad. In the advanced Ca lesions, downregulation of genes related to tumor suppression and those encoding

Table 4. List of representative genes with known functional annotations associated with carcinogenesis showing altered expression in common with all types of thyroid proliferative lesions induced in rats using a two-stage thyroid carcinogenesis model (≥2-fold, ≤0.5-fold)†

Gene function	Accession no.	Gene title	Symbol	FFCH + Ad	Ca
Upregulated genes (of 93 genes in total)					
Adhesion	AA945643	Chitinase 3-like 1	Chi3l1	7.46	8.55
Adhesion	AI169104	Platelet factor 4	Pf4	2.52	3.71
Angiogenesis	NM_021751	Prominin 1	Prom1	4.26	5.53
Transport	NM_012532 (AF202115)	Ceruloplasmin	Cp	3.32 (2.43)	4.12 (2.79)
Transport	AA901341	Solute carrier family 2 (facilitated glucose transporter), member 3	Slc2a3	2.68	2.53
Transport	AA859652 (BG372184)	Solute carrier family 16 (monocarboxylic acid transporters), member 6	Slc16a6	2.28 (2.25)	2.33 (2.24)
Cell proliferation	AF411318	Metallothionein	Mt1a	2.11	3.77
Cell proliferation	AA819913	Carbohydrate (keratan sulfate Gal-6) sulfotransferase 1‡	Chst1	2.77	3.75
Cell proliferation	NM_022278	Glutaredoxin 1 (thioltransferase)	Glrx1	3.63	3.70
Cell proliferation	NM_013122	Insulin-like growth factor binding protein 2	Igfbp2	2.51	2.78
Cell proliferation	AI101583	Transient receptor potential cation channel, subfamily V, member 6	Trpv6	2.01	2.25
Cell proliferation	BI290527	T-box 2‡	Tbx2	2.66	2.19
Biosynthesis	BE097981	Phosphatidylinositol 4-kinase type 2α	Pi4KII	2.66	3.36
Signal transduction	NM_012707	Glucagon	Gcg	3.07	2.79
Cell growth	AW142962	Prolactin receptor	Prlr	2.22	2.46
Tumor progression	BE102969	Ets variant gene 4 (E1A enhancer binding protein, E1AF)‡	Etv4	2.62	2.25
Tumor progression	BG379319	Transforming growth factor, beta induced	Tgfbi	3.41	2.41
Tumor progression	BE120425	Calcium/calmodulin-dependent protein kinase II gamma	Camk2g	2.17	1.90
Cell cycle	NM_133309	Calpain 8	Capn8	2.06	2.55
Cytoskeleton	BE119221	Actinin, α1	Actn1	2.11	2.09
Downregulated genes (of 53 genes in total)					
Adhesion	AW525315 (AI103913)	Poliovirus receptor-related 3‡	Pvrl3	0.46 (0.44)	0.28 (0.31)
Transcription	NM_013060	Inhibitor of DNA binding 2, dominant negative helix-loop-helix protein	Id2	0.47	0.28
Biosynthesis	NM_022276	Glucosaminyl (*N*-acetyl) transferase 1, core 2	Gcnt1	0.44	0.30
Signal transduction	BI276110	Retinoic acid induced 3‡	Rai3	0.48	0.33
Apoptosis	AI227742	Bcl-2-related ovarian killer protein	Bok	0.44	0.36

Ad, adenomas; Ca, carcinomas; FFCH, focal follicular cell hyperplasias.
†Proliferative lesions were divided into two categories, i.e. FFCH + Ad and Ca.
‡Predicted gene identity.

Table 5. Validation of microarray data by real-time reverse transcription-polymerase chain reaction (PCR)

Gene	FFCH + Ad			Ca		
	Microarray	Real-time PCR normalized by		Microarray	Real-time PCR normalized by	
		Hprt	Gapdh		Hprt	Gapdh
Chi3l1	7.40 ± 1.06*	7.35 ± 2.85***	10.73 ± 4.13	8.67 ± 2.67*	8.14 ± 3.49***	14.09 ± 4.61***
Cp	3.29 ± 0.27**	3.18 ± 0.89****	4.69 ± 1.19****	4.12 ± 0.62**	3.50 ± 0.84****	6.15 ± 0.83****
Slc2a3	2.66 ± 0.25**	2.47 ± 0.66****	3.55 ± 0.93	2.52 ± 0.31**	2.41 ± 0.41****	4.15 ± 0.28***
Scl16a6	2.29 ± 0.53**	2.20 ± 0.73***	3.26 ± 1.12****	2.23 ± 0.26**	2.19 ± 0.63***	3.88 ± 0.89****
Gcg	3.07 ± 0.60*	2.37 ± 0.72***	3.46 ± 0.88	2.96 ± 1.21*	2.55 ± 1.17***	4.40 ± 1.69***
Prlr	2.22 ± 0.61*	1.53 ± 0.36	2.21 ± 0.51****	2.51 ± 0.80**	1.87 ± 0.36***	3.23 ± 0.43****
Pi4KII	2.67 ± 0.89*	2.01 ± 0.74	2.96 ± 1.12****	3.30 ± 0.95**	2.17 ± 0.59***	3.84 ± 0.83****
Actn1	2.13 ± 0.47*	1.61 ± 0.48	2.35 ± 0.73****	2.17 ± 0.82*	1.52 ± 0.38	2.67 ± 0.56****
Pvrl3	0.44 ± 0.07*	0.40 ± 0.08	0.59 ± 0.10****	0.31 ± 0.05*	0.35 ± 0.05***	0.62 ± 0.12****
Rai3	0.48 ± 0.06*	0.42 ± 0.06	0.63 ± 0.09****	0.34 ± 0.08*	0.32 ± 0.06***	0.58 ± 0.17****
Gcnt1	0.44 ± 0.08*	0.63 ± 0.14	0.95 ± 0.17	0.31 ± 0.09*	0.37 ± 0.05***	0.67 ± 0.08****

Gapdh, glyceraldehyde 3-phosphate dehydrogenase; Hprt, hypoxanthine-guanine phosphoribosyltransferase.
Values are mean ± SD ($n = 5$) when the expression level in non-tumor follicles was calculated as 1. A single RNA sample for measurement was an equal mixture of total RNA from the same category tissue preparations from two animals.
*,**: Significantly different from non-tumor follicles at $P < 0.05$ and $P < 0.01$, respectively (Student's *t*-test calculated by GeneSpring).
,*: Significantly different from non-tumor follicles at $P < 0.05$ and $P < 0.01$, respectively (Student's *t*-test).

transcriptional inhibitors of Id family proteins appeared specific. These genes may play stage-dependent roles during carcinogenesis. In particular, selective activation of cell-cycle molecules in the early stages is considered to be essential for lesions to undergo efficient replication in response to TSH-stimulation, and loss of tumor-suppressor functions may be necessary for acquisition of a malignant phenotype during the progression stage. As genes upregulated in common in all types of proliferative lesions, we

doi: 10.1111/j.1349-7006.2009.01094.x

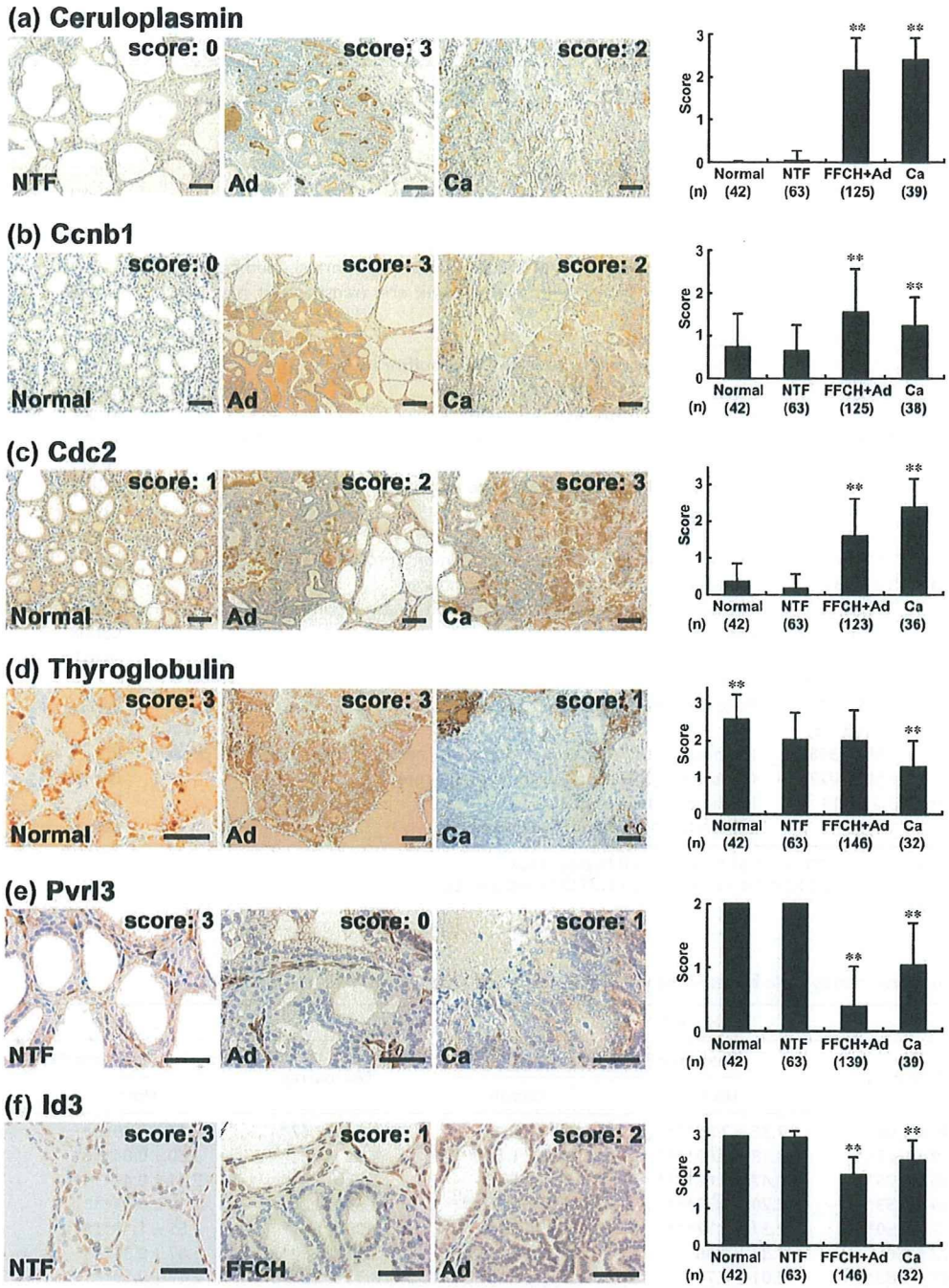

Fig. 2. Immunohistochemical distributions of ceruloplasmin, cyclin B1 (Ccnb1), cell division cycle 2 (Cdc2), thyroglobulin, poliovirus receptor-related 3 (Pvrl3), and inhibitor of DNA binding 3 (Id3) in normal follicular cells of untreated or *N*-bis(2-hydroxypropyl)nitrosamine (DHPN)-treated animals and in proliferative lesions (focal follicular cell hyperplasia [FFCH], adenoma [Ad], carcinoma [Ca]) or surrounding non-tumor follicles (NTF) after promotion with sulfadimethoxine (SDM) for 10 or 15 weeks. (a) Ceruloplasmin in the NTF, Ad, and Ca. Left: NTF nearly lacking ceruloplasmin expression. Middle and right: Ad and Ca showing ceruloplasmin immunoreactivity in the luminal surfaces of cellular membranes of follicular cells. Diffuse or granular immunoreactivity is also evident in the follicular lumina. (b) Ccnb1 in normal follicles, Ad, and Ca. Note fine granular immunoreactivity of Ccnb1 in the cytoplasm of follicular cells. Left: Weak and sparse Ccnb1 localization in normal follicular cells. Middle: Strong and diffuse immunoreactivity in an Ad. Right: Ca demonstrating Ccnb1 immunoreactivity with variable intensity. (c) Cdc2 in normal follicles, Ad, and Ca. Strong Cdc2 immunoreactivity both in the cytoplasm and nucleus of follicular cells. Left: Rather few immunoreactive cells in normal follicles. Middle: An Ad showing sparse Cdc2 immunoreactivity. Right: Note increased numbers of immunoreactive cells in a Ca. (d) Thyroglobulin in normal follicles, Ad, and Ca. Left: Strong and granular thyroglobulin immunoreactivity in the cytoplasm of normal follicular cells as well as diffuse immunoreactivity in the follicular lumina. Middle: Ad showing strong and diffuse thyroglobulin immunoreactivity. Right: A Ca lacking thyroglobulin immunoreactivity in the neoplastic cells. (e) Pvrl3 in the NTF, Ad, and Ca. Left: Diffuse intercellular membrane localization of Pvrl3 in cells comprising NTF. Middle: Ad entirely lacking Pvrl3 expression. Right: Ca showing an irregular and weak intercellular expression pattern. (f) Id3 in NTF, FFCH, and Ad. Left: Diffuse nuclear immunoexpression of Id3 in NTF. Middle: FFCH showing sparse nuclear Id3 expression. Right: Ad showing immunoreactivity in moderate numbers of neoplastic cells. The graphs show scores (mean + SD) for immunohistochemical findings. $^{**}P < 0.01$ versus NTF (Mann–Whitney's *U*-test). (a–f) Scale bar = 50 μm.

also found examples related to cell proliferation, suggesting roles for these molecules consistently throughout carcinogenic processes.

Ceruloplasmin, a copper-containing plasma protein mainly synthesized in the liver, is known to act as a ferroxidase preventing production of toxic Fe and controlling membrane lipid oxidation, while also functioning in angiogenesis and blood coagulation.[19] High levels of antioxidant production likely result from high amounts of reactive oxygen species, which have been implicated in mitogenic signaling and angiogenesis.[27,28] As with high ceruloplasmin levels in the sera of cancer patients, overexpression of ceruloplasmin has been reported in many human malignancies, such as those in the lungs, kidneys, and ovaries.[29–31] With regard to ceruloplasmin in thyroid tumors, it has been demonstrated in follicular cell carcinomas as well as papillary carcinomas, but follicular Ad lack expression.[32–34] In the present study, ceruloplasmin could be immunohistochemically demonstrated in all types of proliferative lesion, in line with transcriptional upregulation. In contrast to the generally benign nature of human Ad, FFCH and Ad in SDM-promoted cases show high cell-proliferation activity similarly to Ca,[9] and this biological behavior may be linked to the increased ceruloplasmin immunoreactivity found in our early proliferative lesions. As discussed by Kondi-Pafiti *et al.*, strong cytoplasmic localization of ceruloplasmin is mainly observed in Ca of human cases, and immunolocalization in luminal secretions (as present in our rat cases) is rare, suggesting a defective catabolism of ceruloplasmin in human Ca.[34]

Cdc2 exerts protein kinase activity by forming complexes with cyclin A2, Ccnb1, and p13suc1 and acts as an active subunit of the M-phase-promoting factor and the M-phase-specific histone H1 kinase.[35] In the present study, increased expression of Ccnb1 and Cdc2, as with other cyclin-related molecules such as cyclin A2, was detected specifically in early proliferative lesions by microarray analysis. Immunohistochemically, we also observed increased expression of Ccnb1 and Cdc2 in both FFCH + Ad and Ca. Chen *et al.* reported coordinated and increased expression of Cdc2 and Ccnb1 in parallel with the pathological grade of human gliomas.[36] They also showed that increased expression of Cdc2 and Ccnb1 contributes to chromosomal instability in tumor cells through alteration of the spindle checkpoint. Thus, the coordinated upregulation of Cdc2 and Ccnb1 observed in the present study might be important as a driving force for both promotion and progression. In another thyroid carcinogenesis study we recently carried out using propylthiouracil as a promoter, a concordant increase of Cdc2 and a cell proliferation marker Ki-67 was found in the proliferative lesions (K. Ago and M. Shibutani, 2008, unpublished data).

Thyroglobulin, a scaffold protein for thyroid hormonogenesis and a storage element for thyroid hormones and iodide, is specifically expressed in the thyroid in response to TSH stimulation.[20] In human malignancies, the presence of thyroglobulin in cancer cells indicates a thyroidal origin.[20] In the present study, although the reason remains unclear, some discrepancy was evident between the mRNA and immunolocalization levels in Ca, the increase in expression on microarray analysis contrasting with the decrease in protein finding. In human thyroid Ca, an inverse relationship between loss of differentiation and thyroglobulin immunoreactivity has been observed, positive cases being less anaplastic,[37] suggesting that the decrease in thyroglobulin in our Ca might have been linked with dedifferentiation, leading to loss of TSH control with malignancy.

Cell adhesion molecules contribute cell-to-cell or cell-to-substratum interactions by homophilic or heterophilic processes.[38] Pvrl molecules, also known as nectins, are adhesion receptors belonging to the IGSF that are involved in cell-to-cell spreading of viruses.[39] Although Pvrl3 protein has not been extensively investigated, it may be a new adhesion molecule expressed on lymphatic endothelial cells.[40] Recent studies have revealed that nectins and nectin-like molecules, in cooperation with integrin and the platelet-derived growth factor receptor, are crucial for mechanisms underlying contact inhibition of cell movement and proliferation.[41] Reduced Pvrl3 expression in all types of proliferative lesions in the present study may reflect acquisition of growth advantage. Interestingly, Pvrl has been shown to be the heterophilic binding partner of another IGSF-type adhesion molecule, tumor suppressor in lung cancer 1 (TSLC1)/IGSF4, a recently identified tumor-suppressor gene.[42,43]

Inhibitor of DNA binding proteins, composed of four members of the helix-loop-helix transcription factors, are known to act as dominant-negative regulators of basic helix-loop-helix transcription factors, and function to inhibit differentiation and enhance cell proliferation.[44,45] In many human malignancies, upregulation of Id has been reported.[46] However, in the present study, all Id isoforms showed downregulation in Ca by microarray analysis, and immunohistochemically, Id3-immunoreactive cells were reduced in all types of proliferative lesions. Similar findings have been reported for human ovarian tumors, in which downregulation of Id3 was noted in 70% of 38 cases.[47] Also, the expression of Id1, Id3, and Id4 was downregulated in microdissected human thyroid Ca compared with surrounding tissues by microarray analysis in one recent study.[48] Although the reason for the inconsistency in the expression alterations between tumor types is not clear, it is possible that gene control mechanisms of Id proteins may differ with the cell type of origin.

In conclusion, we here found differentially regulated genes that may play key roles in early and late stages of thyroid carcinogenesis by microarray analysis of microdissected proliferative lesions developing after promotion with SDM in a two-stage model. Immunohistochemical analysis of representative proliferative lesions indicated facilitation of the cell cycle in early lesions by forming an M-phase promoting factor, as evidenced by the synchronized localization of Ccnb1 and Cdc2, and generation of oxidative stress responses by ceruloplasmin accumulation, as well as reduction of cellular adhesion involving Pvrl3 and cellular differentiation related to transcriptional control by Id3. Decreased expression of thyroglobulin in Ca may reflect dedifferentiation. Although further studies should address particular roles in the processes of thyroid carcinogenesis, the molecules identified in the present study provide pointers to understanding the mechanism of non-genotoxic carcinogenesis and should help in efforts to secure human health.

Acknowledgments

We thank Miss Tomomi Morikawa and Ayako Kaneko for their technical assistance in conducting the animal study. This work was supported by Health and Labour Sciences Research Grants (Research on Food Safety) from the Ministry of Health, Labour, and Welfare of Japan. We all authors disclose here that there are no conflicts of interest that could inappropriately influence the outcome of the present study.

References

1 Thyroid Carcinoma Task Force. AACE/AAES medical/surgical guidelines for clinical practice: management of thyroid carcinoma. American Association of Clinical Endocrinologists. American College of Endocrinology. *Endocr Pract* 2001; **7**: 202–20.

2 Schneider AB, Sarne DH. Long-term risks for thyroid cancer and other neoplasms after exposure to radiation. *Nat Clin Pract Endocrinol Metab* 2005; **1**: 82–91.

3 Kitahori Y, Hiasa Y, Konishi N, Enoki N, Shimoyama T, Miyashiro A. Effect of propylthiouracil on the thyroid tumorigenesis induced by *N*-bis (2-hydroxypropyl) nitrosamine in rats. *Carcinogenesis* 1984; **5**: 657–60.

doi: 10.1111/j.1349-7006.2009.01094.x

4 Jemec B. Studies of the goitrogenic and tumorigenic effect of two goitrogens in combination with hypophysectomy or thyroid hormone treatment. *Cancer* 1980; **45**: 2138–48.
5 Hiasa Y, Ohshima M, Kitahori Y, Yuasa T, Fujita T, Iwata C. Promoting effects of 3-amino-1,2,4-triazole on the development of thyroid tumors in rats treated with *N*-bis (2-hydroxypropyl) nitrosamine. *Carcinogenesis* 1982; **3**: 381–4.
6 Hard GC. Recent developments in the investigation of thyroid regulation and thyroid carcinogenesis. *Environ Health Perspect* 1998; **106**: 427–36.
7 Smith P, Williams ED, Wynford-Thomas D. *In vitro* demonstration of a TSH-specific growth desensitising mechanism in rat thyroid epithelium. *Mol Cell Endocrinol* 1987; **51**: 51–8.
8 Brewer C, Yeager N, Di Cristofano A. Thyroid-stimulating hormone initiated proliferative signals converge *in vivo* on the mTOR kinase without activating AKT. *Cancer Res* 2007; **67**: 8002–6.
9 Mitsumori K, Onodera H, Takahashi M *et al.* Effect of thyroid stimulating hormone on the development and progression of rat thyroid follicular cell tumors. *Cancer Lett* 1995; **92**: 193–202.
10 Roy G, Mugesh G. Bioinorganic chemistry in thyroid gland: effect of antithyroid drugs on peroxidase-catalyzed oxidation and iodination reactions. *Bioinorg Chem Appl* 2006; **2006**: 23214.
11 Shibutani M, Uneyama C, Miyazaki K, Toyoda K, Hirose M. Methacarn fixation: a novel tool for analysis of gene expressions in paraffin-embedded tissue specimens. *Lab Invest* 2000; **80**: 199–208.
12 Uneyama C, Shibutani M, Masutomi N, Takagi H, Hirose M. Methacarn fixation for genomic DNA analysis in microdissected, paraffin-embedded tissue specimens. *J Histochem Cytochem* 2002; **50**: 1237–45.
13 Takagi H, Shibutani M, Kato N *et al.* Microdissected region-specific gene expression analysis with methacarn-fixed, paraffin-embedded tissues by real-time RT-PCR. *J Histochem Cytochem* 2004; **52**: 903–13.
14 Takagi H, Shibutani M, Lee KY *et al.* Impact of maternal dietary exposure to endocrine-acting chemicals on progesterone receptor expression in microdissected hypothalamic medial preoptic areas of rat offspring. *Toxicol Appl Pharmacol* 2005; **208**: 127–36.
15 Shibutani M, Lee KY, Igarashi K *et al.* Hypothalamus region-specific global gene expression profiling in early stages of central endocrine disruption in rat neonates injected with estradiol benzoate or flutamide. *Dev Neurobiol* 2007; **67**: 253–69.
16 Lee KY, Shibutani M, Inoue K, Kuroiwa KUM, Woo GH, Hirose M. Methacarn fixation – effects of tissue processing and storage conditions on detection of mRNAs and proteins in paraffin-embedded tissues. *Anal Biochem* 2006; **351**: 36–43.
17 Hardisty JF, Boorman GA. Thyroid gland. In: Boorman GA, Eustis SL, Elwell MR, Montgomery CA Jr, MacKenzie WF, eds. *Pathology of the Fischer Rat, Reference and Atlas*. San Diego: Academic Press, 1990: 519–36.
18 Imai T, Onose J, Hasumura M, Ueda M, Takizawa T, Hirose M. Sequential analysis of development of invasive thyroid follicular cell carcinomas in inflamed capsular regions of rats treated with sulfadimethoxine after *N*-bis (2-hydroxypropyl) nitrosamine-initiation. *Toxicol Pathol* 2004; **32**: 229–36.
19 Goldstein IM, Kaplan HB, Edelson HS, Weissmann G. Ceruloplasmin. A scavenger of superoxide anion radicals. *J Biol Chem* 1979; **254**: 4040–5.
20 Lin JD. Thyroglobulin and human thyroid cancer. *Clin Chim Acta* 2008; **388**: 15–21.
21 Ziak M, Meier M, Novak-Hofer I, Roth J. Ceruloplasmin carries the anionic glycan oligo/poly α2,8 deaminoneuraminic acid. *Biochem Biophys Res Commun* 2002; **295**: 597–602.
22 Scott IS, Morris LS, Bird K *et al.* A novel immunohistochemical method to estimate cell-cycle phase distribution in archival tissue: implications for the prediction of outcome in colorectal cancer. *J Pathol* 2003; **201**: 187–97.
23 Yamamoto H, Monden T, Ikeda K *et al.* Coexpression of cdk2/cdc2 and retinoblastoma gene products in colorectal cancer. *Br J Cancer* 1995; **71**: 1231–6.
24 Faggiano A, Caillou B, Lacroix L *et al.* Functional characterization of human thyroid tissue with immunohistochemistry. *Thyroid* 2007; **17**: 203–11.
25 Kuramitsu K, Ikeda W, Inoue N, Tamaru Y, Takai Y. Novel role of nectin: implication in the co-localization of JAM-A and claudin-1 at the same cell–cell adhesion membrane domain. *Genes Cells* 2008; **13**: 797–805.
26 Carroll M, Hamzeh M, Robaire B. Expression, localization, and regulation of inhibitor of DNA binding (Id) proteins in the rat epididymis. *J Androl* 2006; **27**: 212–24.
27 Lelkes PI, Hahn KL, Sukovich DA, Karmiol S, Schmidt DH. On the possible role of reactive oxygen species in angiogenesis. *Adv Exp Med Biol* 1998; **454**: 295–310.
28 Suh YA, Arnold RS, Lassegue B *et al.* Cell transformation by the superoxide-generating oxidase Mox1. *Nature* 1999; **401**: 79–82.
29 Stassar MJ, Devitt G, Brosius M *et al.* Identification of human renal cell carcinoma associated genes by suppression subtractive hybridization. *Br J Cancer* 2001; **85**: 1372–82.
30 Hough CD, Cho KR, Zonderman AB, Schwartz DR, Morin PJ. Coordinately up-regulated genes in ovarian cancer. *Cancer Res* 2001; **61**: 3869–76.
31 Wang KK, Liu N, Radulovich N *et al.* Novel candidate tumor marker genes for lung adenocarcinoma. *Oncogene* 2002; **21**: 7598–604.
32 Tuccari G, Barresi G. Immunohistochemical demonstration of ceruloplasmin in follicular adenomas and thyroid carcinomas. *Histopathology* 1987; **11**: 723–31.
33 Song B. Immunohistochemical demonstration of epidermal growth factor receptor and ceruloplasmin in thyroid diseases. *Acta Pathol Jpn* 1991; **41**: 336–43.
34 Kondi-Pafiti A, Smyrniotis V, Frangou M, Papayanopoulou A, Englezou M, Deligeorgi H. Immunohistochemical study of ceruloplasmin, lactoferrin and secretory component expression in neoplastic and non-neoplastic thyroid gland diseases. *Acta Oncol* 2000; **39**: 753–6.
35 Draetta G, Luca F, Westendorf J, Brizuela L, Ruderman J, Beach D. cdc2 protein kinase is complexed with both cyclin A and B. Evidence for proteolytic inactivation of MPF. *Cell* 1989; **56**: 829–38.
36 Chen H, Huang Q, Dong J, Zhai DZ, Wang AD, Lan Q. Overexpression of CDC2/CyclinB1 in gliomas, and CDC2 depletion inhibits proliferation of human glioma cells *in vitro* and *in vivo*. *BMC Cancer* 2008; **8**: 29.
37 Wiseman SM, Griffith OL, Deen S *et al.* Identification of molecular markers altered during transformation of differentiated into anaplastic thyroid carcinoma. *Arch Surg* 2007; **142**: 717–29.
38 Simmons DL. Dissecting the modes of interactions amongst cell adhesion molecules. *Dev Suppl* 1993; **???**: 193–203.
39 Geraghty RJ, Krummenacher C, Cohen GH, Eisenberg RJ, Spear PG. Entry of alphaherpesviruses mediated by poliovirus receptor-related protein 1 and poliovirus receptor. *Science* 1998; **280**: 1618–20.
40 Nelson GM, Padera TP, Garkavtsev I, Shioda T, Jain RK. Differential gene expression of primary cultured lymphatic and blood vascular endothelial cells. *Neoplasia* 2007; **9**: 1038–45.
41 Takai Y, Miyoshi J, Ikeda W, Ogita H. Nectins and nectin-like molecules: roles in contact inhibition of cell movement and proliferation. *Nat Rev Mol Cell Biol* 2008; **9**: 603–15.
42 Murakami Y. Involvement of a cell adhesion molecule, TSLC1/IGSF4, in human oncogenesis. *Cancer Sci* 2005; **96**: 543–52.
43 Wakayama T, Sai Y, Ito A *et al.* Heterophilic binding of the adhesion molecules poliovirus receptor and immunoglobulin superfamily 4A in the interaction between mouse spermatogenic and Sertoli cells. *Biol Reprod* 2007; **76**: 1081–90.
44 Benezra R, Davis RL, Lockshon D, Turner DL, Weintraub H. The protein Id. A negative regulator of helix-loop-helix DNA binding proteins. *Cell* 1990; **61**: 49–59.
45 Ellis HM, Spann DR, Posakony JW. *Extramacrochaetae*, a negative regulator of sensory organ development in *Drosophila*, defines a new class of helix-loop-helix proteins. *Cell* 1990; **61**: 27–38.
46 Sikder HA, Devlin MK, Dunlap S, Ryu B, Alani RM. Id proteins in cell growth and tumorigenesis. *Cancer Cell* 2003; **3**: 525–30.
47 Arnold JM, Mok SC, Purdie D, Chenevix-Trench G. Decreased expression of the *Id3* gene at 1p36.1 in ovarian adenocarcinomas. *Br J Cancer* 2001; **84**: 352–9.
48 Nikolova DN, Zembutsu H, Sechanov T *et al.* Genome-wide gene expression profiles of thyroid carcinoma: Identification of molecular targets for treatment of thyroid carcinoma. *Oncol Rep* 2008; **20**: 105–21.

Supporting Information

Additional Supporting Information may be found in the online version of this article:

Table S1. List of genes showing altered expression in microdissected focal follicular cell hyperplasias (FFCH) + adeomas (Ad) induced in the thyroids of rats using a two-stage thyroid carcinogenesis model (≥2-fold, ≤0.5-fold).

Table S2. List of genes showing altered expression in microdissected carinomas (Ca) induced in the thyroid of rats using a two-stage thyroid carcinogenesis model (≥2-fold, ≤0.5-fold).

Table S3. List of genes showing altered expression in common in all types of thyroid proliferative lesion induced in rats using a two-stage thyroid carcinogenesis model (≥2-fold, ≤0.5-fold).

Please note: Wiley-Blackwell are not responsible for the content or functionality of any supporting materials supplied by the authors. Any queries (other than missing material) should be directed to the corresponding author for the article.

Neonatal Exposure to Low-Dose 2,3,7,8-Tetrachlorodibenzo-*p*-Dioxin Causes Autoimmunity Due to the Disruption of T Cell Tolerance[1]

Naozumi Ishimaru,* Atsuya Takagi,† Masayuki Kohashi,* Akiko Yamada,* Rieko Arakaki,* Jun Kanno,† and Yoshio Hayashi[2]*

Although 2,3,7,8-tetrachlorodibenzo-*p*-dioxin (TCDD) has been shown to influence immune responses, the effects of low-dose TCDD on the development of autoimmunity are unclear. In this study, using NFS/*sld* mice as a model for human Sjögren's syndrome, in which the lesions are induced by the thymectomy on day 3 after birth, the autoimmune lesions in the salivary glands, and in later phase, inflammatory cell infiltrations in the other organs were developed by neonatal exposure to nonapoptotic dosage of TCDD without thymectomy on day 3 after birth. We found disruption of thymic selection, but not thymic atrophy, in TCDD-administered mice. The endogenous expression of aryl hydrocarbon receptor in the neonatal thymus was significantly higher than that in the adult thymus, suggesting that the neonatal thymus may be much more sensitive to TCDD compared with the adult thymus. In addition, the production of T_H1 cytokines such as IL-2 and IFN-γ from splenic $CD4^+$ T cells and the autoantibodies relevant for Sjögren's syndrome in the sera from TCDD-exposed mice were significantly increased compared with those in control mice. These results suggest that TCDD/aryl hydrocarbon receptor signaling in the neonatal thymus plays an important role in the early thymic differentiation related to autoimmunity. *The Journal of Immunology*, 2009, 182: 6576–6586.

The toxicity of 2,3,7,8-tetrachlorodibenzo-*p*-dioxin (TCDD),[3] the environmental contaminant, has been shown to influence various biological responses such as immunological, reproductive, and neurobehavioral (1–3). It has been reported that TCDD induces thymic atrophy and suppresses a variety of T cell-dependent immune responses, including delayed-type and contact hypersensitivity responses and the activity of CTL itself (4–7). However, TCDD has been shown to enhance the proliferation and cytokine production of mitogen- or Ag-stimulated T cells (8). In this context, when a DO11.10 transgenic T cell model was used to investigate the effects of TCDD on the activation of Ag-specific $CD4^+$ T cells by transfer of $CD4^+$ T cells into TCDD-treated recipient mice, the exposure to TCDD had little effect on the initial activation, but on day 3 after OVA-peptide injection the T cell proliferation of TCDD-treated recipients was enhanced compared with that of control recipients (9). Thus, the effect of TCDD seems to be dependent on the developmental state and active state of the T cells. As for the effects of TCDD on B cells, it was reported that TCDD inhibited B cell proliferation triggered by LPS, surface Ig cross-linking, or PMA/ionomycin (10, 11). Moreover, the in vivo suppressive effect of TCDD on T cell-dependent Ab response to sheep RBC (SRBC) was found as an immunotoxicity of TCDD (12). However, the effects of TCDD on autoimmunity or on autoantibody production in autoimmune animal models have not been demonstrated.

A combination of immunologic, genetic, and environmental factors may play a key role on the development of autoimmune disease, which is induced by the breakdown of central or peripheral tolerance (13–15). Sjögren's syndrome (SS) is generally considered to be a T cell-mediated autoimmune disorder characterized by lymphocytic infiltrates and destruction of the exocrine glands, particularly of the salivary glands, and systemic production of autoantibodies against the ribonucleoprotein particles SS-A/Ro and SS-B/La (16–18). We have established and analyzed an animal model for SS in NFS/*sld* mutant mouse thymectomized 3 days after birth (3d-Tx) (19–21). It is well established that 3d-Tx in a certain strain of mice results in spontaneous development of inflammatory lesions similar to human autoimmune diseases in the thyroid, ovary, kidney, testis, and stomach, but little is known about the mechanisms leading to the induction of autoimmunity (22–25). From the findings in 3d-Tx autoimmune models, the initiation of autoreactivity is thought to be due to the retardation of regulatory T (Treg) cell differentiation together with lymphopenia caused by neonatal thymectomy. In other words, the impairment of T cell differentiation and/or maturation in the neonatal thymus may cause the initiation of T cell self-reactivity. Although the perinatal exposure to TCDD has been shown to induce the suppression of cell-mediated immunity to a more severe degree than those in adult exposure, the association of neonatal exposure to TCDD with the development of autoimmunity remains unclear (5, 6).

*Department of Oral Molecular Pathology, Institute of Health Biosciences, University of Tokushima Graduate School, Kuramotocho, Tokushima, Japan; and †Division of Cellular and Molecular Toxicology, Biological Safety Research Center, National Institute of Health Sciences, Kamiyoga, Setagayaku, Tokyo, Japan

Received for publication July 14, 2008. Accepted for publication March 17, 2009.

The costs of publication of this article were defrayed in part by the payment of page charges. This article must therefore be hereby marked *advertisement* in accordance with 18 U.S.C. Section 1734 solely to indicate this fact.

[1] This work was supported by a Health Sciences Research Grant (H17, 18, and 19-kagaku-ippan-003) from the Ministry of Health, Labor and Welfare, Japan and a Grant-in-Aid for Scientific Research (no. 17109016) from the Ministry of Education, Culture, Sports, Science and Technology of Japan.

[2] Address correspondence and reprint requests to Dr. Yoshio Hayashi, Department of Oral Molecular Pathology, Institute of Health Biosciences, University of Tokushima Graduate School, 3-18-15 Kuramotocho, Tokushima 770-8504, Japan. E-mail address: hayashi@dent.tokushima-u.ac.jp

[3] Abbreviations used in this paper: TCDD, 2,3,7,8-tetrachlorodibenzo-*p*-dioxin; 3d-Tx, thymectomized 3 days after birth; AhR, aryl hydrocarbon receptor; AIRE, autoimmune regulator; ARNT, AhR nuclear translocator; DN, double negative; DP, double positive; DRE, dioxin responsive element; IRF, IFN regulatory factor; SP, single positive; SS, Sjögren's syndrome; TEC, thymic epithelial cell; Treg, regulatory T; XRE, xenobiotic response element.

www.jimmunol.org/cgi/doi/10.4049/jimmunol.0802289

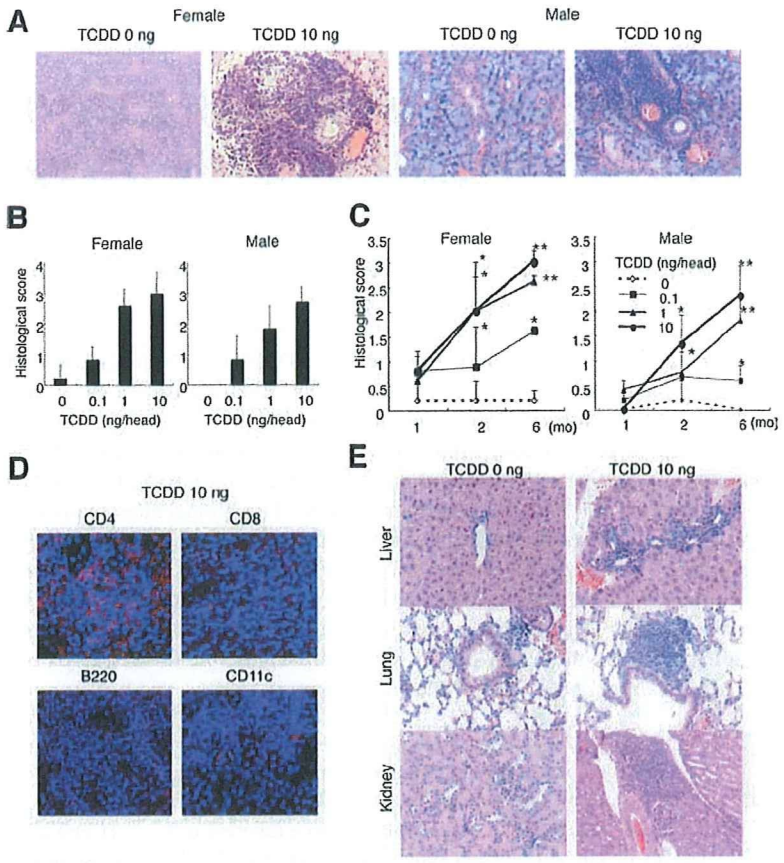

FIGURE 1. Inflammatory lesions induced by neonatal exposure to low-dose TCDD. *A*, Histology of salivary glands in female and male mice (6 mo) treated with 0 and 10 ng of TCDD were shown. H&E staining was performed using paraffin-embedded sections. Photos are representative of five to seven mice in each group. *B*, Histological score of the salivary glands at 6 mo of age was evaluated using the sections stained with H&E. Results are shown as the mean ± SD in the five to seven mice in each group. *C*, The change of inflammatory lesions from 1 to 6 mo of age in female and male mice treated with low-dose TCDD. Results are shown as the mean ± SD in the five to seven mice in each group. *, $p < 0.05$; **, $p < 0.005$. *D*, Immune cells in the inflammatory lesions of salivary glands from TCDD-treated mice at 6 mo of age were analyzed by immunofluorescence staining using anti-CD4, CD8, B220, and CD11c mAbs with Alexa Fluor 568-conjugated rat IgG (H+L) as the secondary Abs. Nuclei were stained with 4′,6-diamidino-2-phenylindole. Photos are representative of three to five sections in each group. *E*, Inflammatory lesions of liver, lung, and kidney induced by TCDD treatment. The sections from TCDD-treated mice at 6 mo of age were stained with H&E. Photos are representative of five to seven mice in each group.

One mechanism of TCDD action is binding and activation of the aryl hydrocarbon receptor (AhR) (1, 26). The AhR is a cytosolic transcription factor of the basic helix-loop-helix family. The activated receptor heterodimerizes with the AhR nuclear translocator (ARNT) in the nucleus and binds the xenobiotic response elements (XREs), also known as dioxin responsive elements (DREs), and alters the expressions of various genes such as cytochrome P450 1A1 (CYP1A1). TCDD, via the AhR, has been shown to have a variety of effects on T cell development and function, including decreasing the number of thymocytes by apoptosis and altering the effector functions of mature Th and T killer cells (27–30). Although a variety of studies have been performed to determine how high-dose TCDD is influencing T cells and the thymus (29–31), the mechanism and targets of its actions are still unclear. In addition, TCDD also induced the binding of several NF-κB proteins to a κB site, one of which overlapped with a DRE site (32). It has been uncertain whether the neonatal exposure to low-dose TCDD in vivo influences the TCDD signaling including AhR, CYP1A1, or NF-κB of immune cells.

In this study, we evaluated whether the immunotoxicity of nonapoptotic and low-dose TCDD during neonatal period influences the development of autoimmune disease in the murine SS-susceptible strain. Moreover, the correlation between the TCDD-induced signaling pathway in neonatal T cells and the initiation of self-reactivity in vivo was analyzed.

Materials and Methods

Mice

NFS/N strain carrying the mutant gene *sld* was reared in our specific pathogen-free mouse colony, and given food and water ad libitum. Experiments were humanely conducted under the regulation and permission of the Animal Care and Use Committee of the National Institute of Health Sciences, Tokyo, Japan and the University of Tokushima, Tokushima, Japan.

Neonatal administration of TCDD

Intraperitoneal injection of 10 μl of corn oil including TCDD (0, 0.1, 1, or 10 ng/mouse) with neonatal mice was performed on day 0, 1, and 2 after birth. Treatment of TCDD and TCDD-injected mice followed the rules of the National Institute of Health Sciences.

Histology

All organs were removed from the mice, fixed with 4% phosphate-buffered formaldehyde (pH 7.2), and prepared for histologic examination. Formalin-fixed tissue sections were subjected to H&E staining, and three pathologists independently evaluated the histology without being informed of the condition of each individual mouse. Histological changes were scored according to the method proposed by White and Casarett (33), as follows: 1 = 1–5 foci composed of >20 mononuclear cells per focus; 2 = >5 such foci, but without significant parenchymal destruction; 3 = degeneration of parenchymal tissue; 4 = extensive infiltration of the glands with mononuclear cells and extensive parenchymal destruction. Histological evaluation was performed in a blinded manner, and one tissue section from each salivary and lacrimal gland was examined.

Confocal microscopic analysis

Frozen sections were stained with 1 μg/ml primary Abs against CD4, CD8, B220, and CD11b/c (eBioscience) for 1 h. After three washes in PBS, the sections were stained with Alexa Fluor 568 donkey anti-rat IgG (H+L) (Molecular Probes) as the second Abs for 30 min and washed with PBS. The nuclei was stained with 4′,6-diamidino-2-phenylindole. The sections were visualized with a laser scanning confocal microscope (Carl Zeiss). A 63 × 1.4 oil differential interference contrast objective lens was used. Quick Operation Version 3.2 (Carl Zweiss) for imaging acquisition and Adobe Photoshop CS2 (Adobe System) for image processing was used.

Table I. *Incidence of inflammatory lesions in TCDD-treated mice*

	Female			Male		
	1 mo	2 mo	6 mo	1 mo	2 mo	6 mo
Liver treated with TCDD (ng)						
0	0/5 (0)	0/7 (0)	0/5 (0)	0/6 (0)	0/6 (0)	0/9 (0)
0.1	0/6 (0)	2/8 (25)	2/5 (40)	0/5 (0)	0/6 (0)	2/6 (33)
1	1/5 (20)	2/6 (33)	1/6 (17)	4/8 (50)	0/6 (0)	2/6 (33)
10	2/5 (40)	3/6 (50)	2/6 (33)	2/6 (33)	4/6 (67)	5/7 (71)
Lung treated with TCDD (ng)						
0	0/5 (0)	0/7 (0)	1/6 (17)	0/6 (0)	0/7 (0)	0/9 (0)
0.1	0/6 (0)	4/8 (50)	3/5 (60)	0/5 (0)	0/5 (0)	3/6 (50)
1	1/5 (20)	2/6 (33)	4/6 (67)	2/8 (25)	3/6 (50)	6/6 (100)
10	2/5 (40)	3/6 (50)	6/6 (100)	1/6 (17)	6/6 (100)	7/7 (100)
Kidney treated with TCDD (ng)						
0	0/5 (0)	0/7 (0)	0/6 (0)	0/6 (0)	0/7 (0)	0/9 (0)
0.1	0/6 (0)	0/8 (0)	1/5 (20)	1/5 (20)	3/5 (60)	4/6 (67)
1	0/5 (0)	0/6 (0)	2/6 (33)	2/8 (25)	4/6 (67)	5/6 (83)
10	1/5 (20)	3/6 (50)	2/6 (33)	2/6 (33)	6/6 (100)	5/7 (71)

The incidence of inflammatory lesions in the liver, lung, and kidney was histologically evaluated using the H&E-stained sections of the TCDD-treated NFS/*sld* mice at 1, 2, and 6 mo of age. The number of inflammatory lesion-induced mice in the organ/the total number of treated mice (%) is indicated.

Flow cytometric analysis

Surface markers were identified by mAbs with BD FACSCant flow cytometer (BD Biosciences). Rat mAbs to FITC-, PE-, or PE-Cy5-conjugated anti-B220, Thy1.2, CD4, CD8, CD25, and CD44 mAbs (eBioscience) were used. Intracellular Foxp3 expression was analyzed with an intracellular Foxp3 detection kit (eBioscience) according to the manufacturer's instructions. For intracellular AhR expression, cells were stained with PE-Cy5.5-conjugated anti-CD4, PE-conjugated anti-CD8, PE-Cy7-conjugated anti-CD44, allophycocyanin-conjugated anti-CD25 mAbs, and then fixed in fixation/permeabilization solution (eBioscience) for 18 h at 4°C. After washing twice with the permeabilization buffer (eBioscience), the cells were blocked with Fc block for 40 min on ice, and incubated in rabbit anti-AhR polyclonal Ab (BIOMOL) for 2 h at 4°C. After washing with the permeabilization buffer, the cells were stained with FITC-conjugated ant-rabbit IgG for 30 min at 4°C for flow cytometric analysis of multicolors. The data were analyzed with FlowJo FACS Analysis software (Tree Star).

Proliferation assay

Cell proliferation was evaluated by counting of divisions by CFSE (Molecular Probes) dilution of labeled cells. After stimulation by anti-CD3 and

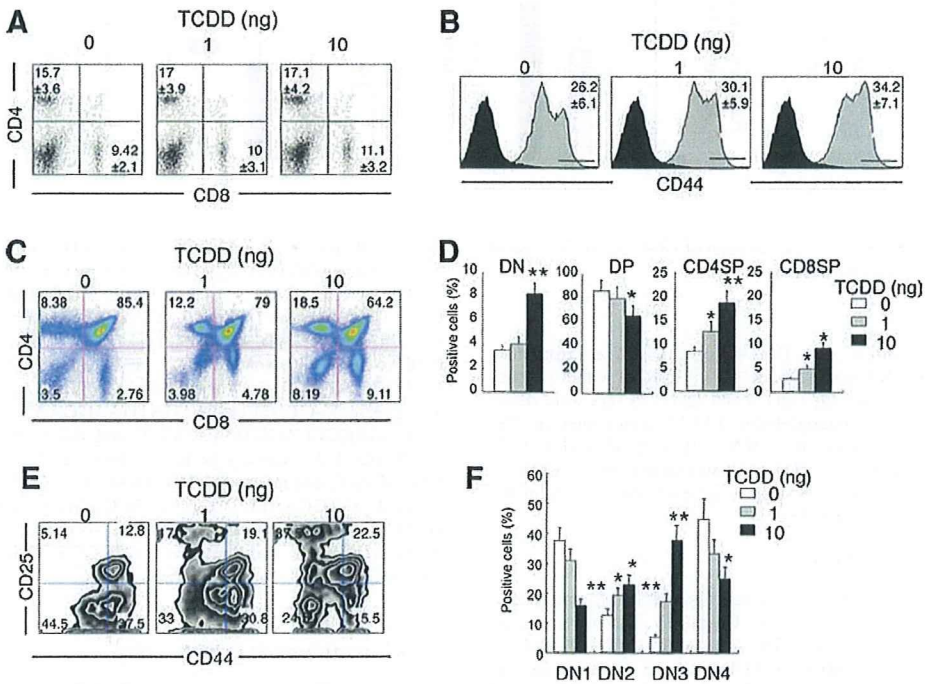

FIGURE 2. The effect of in vivo TCDD injection on T cell phenotypes. *A*, CD4 and CD8 expressions on spleen cells from female TCDD-treated mice at 6 mo of age were analyzed by flow cytometry. Positive cells (%) were indicated as the mean ± SD of five to seven mice in each group. *B*, CD44 expression on $CD4^+$ T cells in spleen from TCDD-treated mice. $CD44^{high}$ cells (%) are indicated as the mean ± SD of five to seven mice in each group. *C*, T cell differentiation in thymus of TCDD-treated mice was analyzed by flow cytometry using CD4 and CD8 expressions. Figures are representative of five to seven mice in each group. *D*, T cell population in thymus. $CD4^-CD8^-$ DN, $CD4^+CD8^+$ DP, $CD4^+CD8^-$ SP (CD4SP), and $CD4^-CD8^+$ SP (CD8SP) cells (%) are shown as the mean ± SD of five to seven mice in each group. *E*, The differentiation of DN T cells was evaluated using CD44 and CD25 expressions. Figures are representative of five to seven mice in each group. *F*, $CD44^+CD25^-$ (DN1), $CD44^+CD25^+$ (DN2), $CD44^-CD25^+$ (DN3), and $CD44^-CD25^-$ (DN4) cells (%) are shown as the mean ± SD of five to seven mice in each group. *, $p < 0.05$; **, $p < 0.005$.

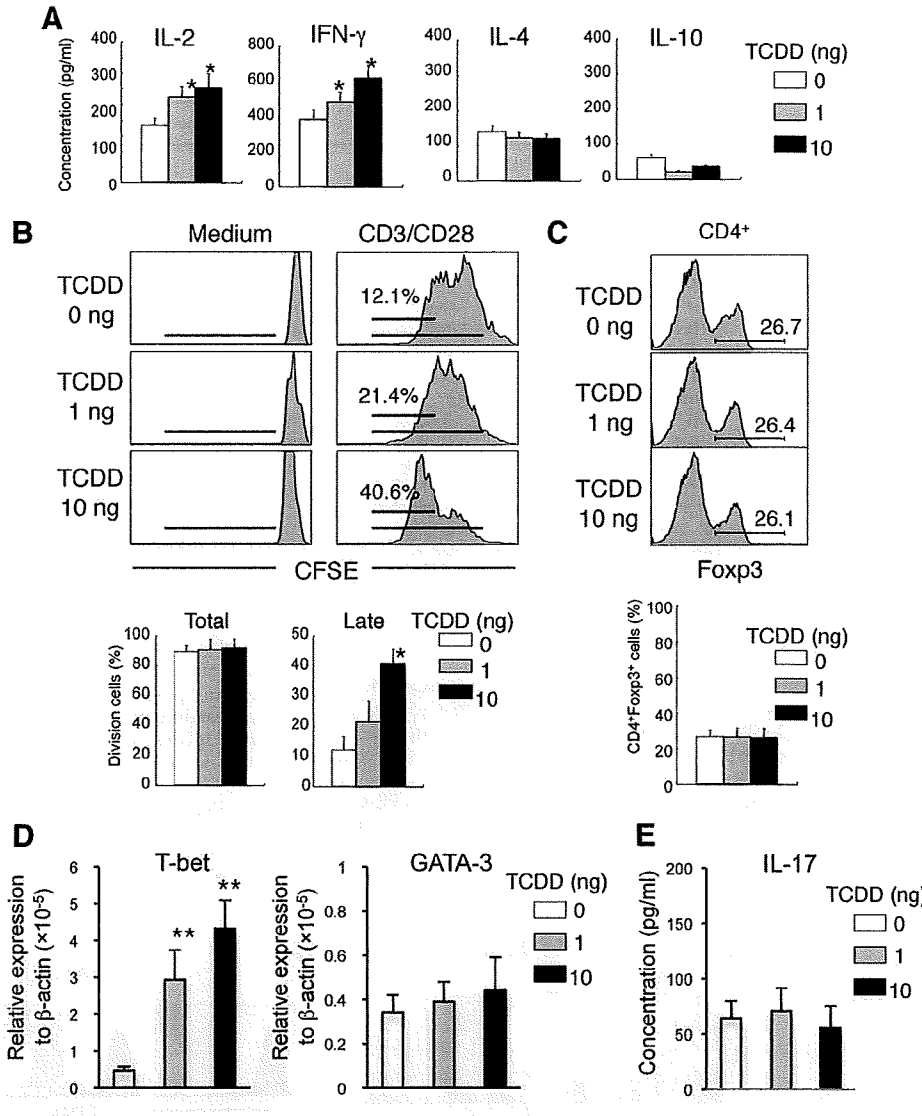

FIGURE 3. T cell functions in low-dose TCDD-treated mice. *A*, T_H1 and T_H2 type cytokine productions were analyzed by ELISA using the culture supernatants from splenic T cell-stimulated plate-coated anti-CD3 mAb for 24 h. Results are shown as mean ± SD of triplicates and representative of four to five mice in each group. *B*, Proliferative response of splenic T cell-stimulated plate-coated anti-CD3 and CD28 mAbs from TCDD-treated mice was analyzed with CFSE dilutions during 72 h. Results are representative of three to five mice in each group. *C*, $Foxp3^+CD4^+$ Treg cells in spleen from TCDD-treated mice were analyzed by flow cytometry. Results are representative of three to five mice in each group. $Foxp3^+$ cells (%) are indicated as mean ± SD of three to five mice in each group. *, $p < 0.05$. *D*, T-bet and GATA-3 mRNA expressions of spleen from TCDD-treated mice were detected by real-time PCR. Data are shown as mean ± SD of four to six mice per each group. *, $p < 0.05$; **, $p < 0.005$. *E*, IL-17 production was analyzed by ELISA using the culture supernatants from splenic T cell-stimulated plate-coated anti-CD3 mAb for 24 h. Results are shown as mean ± SD of triplicates and representative of four mice in each group.

anti-CD28 mAbs, or LPS for 72 h, cell division of $CD4^+$ or $B220^+$-gated spleen cells was analyzed by flow cytometry.

ELISA

The JS-1-, SS-A/Ro-, SS-B/La-, or ss-DNA-specific Abs of sera from mice were measured by an ELISA reader (model 680; Bio-Rad) with a spectrophotometer reading at 490 nm. Igs (IgG2a and IgG1) in sera were determined by using the mouse immunoglobulins ELISA quantitation kit (Bethyl Laboratories). For detection of IL-2, IFN-γ, IL-4, IL-10, and IL-17 in the culture supernatants from anti-CD3 mAb-stimulated splenic $CD4^+$ T cells for 24 h, ELISA were performed by using each specific Ab for the cytokines as previously described (34).

Real-time quantitative RT-PCR

Total RNA was extracted from thymus, spleen, and cultured thymocytes in NFS/*sld* mice using Isogen (Wako Pure Chemical), and reverse transcribed. Transcript levels of T-bet, GATA-3, AhR, CYP1A1, Bcl-xL, TNF-α, IFN regulatory factor (IRF)-1, GADD45, IL-1β, autoimmune regulator (AIRE), salivary protein-1, GAD67, and β-actin were performed using DNA Engine OPTICOM system (Bio-Rad) with SYBR Premix Ex Tag (Takara Shuzo). Primer sequences were as follows: T-bet: forward, 5′-CCTGTTGTGGTCCAAGTTCAAC-3′ and reverse, 5′-CACAAACAT CCTGTAATGGCTTGT-3′; GATA-3: forward, 5′-GACTTGCCAGAAAG GCAGAC-3′, and reverse, 5′-AAAGAGGTCACCACCCACAG-3′; AhR: forward, 5′-ACATAACGGACGAAATCCTGACC-3′ and reverse, 5′-TC AACTCTGCACCTTGCTTAGGA-3′; CYP1A1: forward, 5′-CCATGACC GGGAACTGTGG-3′, and reverse, 5′-TCTGGTGAGCATCCTGGACA-3′; NF-κB: forward, 5′-ATGGCAGACGATGATCCCTA-3′ and reverse, 5′-TAGGCAAGGTCAGAATGCAC-3′; Bcl-xL: forward, 5′-AGAAGA AACTGAAGCAGAG-3′, and reverse, 5′-TCCGACTCACCAATACCT G-3′; TNF-α, forward, 5′-ATGAGCACAGAAAGCATGATC-3′, and reverse, 5′-AGATGATCTGAGTGTGAGGG-3′; GADD45: forward, 5′-TG GTGACGAACCCACATTCAT-3′, and reverse, 5′-ACCCACTGATCCAT GTAGCGAC-5′; IL-1β: forward, 5′-TGATGAGAATGACCTGTTCT-3′, and reverse, 5′-CTTCTTCAAAGATGAAGGAAA-3′; AIRE: forward, 5′-AAGGGAGCCCAGGTCACTAT-3′, and reverse, 5′-ATTGAGGAGGGA CTCCAGGT-3′; salivary protein-1: forward, 5′-GGCTCTGAAACTCA GGCAGA-3′, and reverse, 5′-TGCAAACTCATCCACGTTGT-3′; GAD67: forward, 5′-TGCAACCTCCTCGAACGCGG-3′, and reverse, 5′-CCAG GATCTGCTCCAGAGAC-3′; β-actin: forward, 5′-GTGGGCCGCTCT AGGCACCA-3′ and reverse, 5′-CGGTTGGCCTTAGGGTTCAG GGGGG-3′.

NF-κB transcription activity assay

The transcriptional activity of NF-κB of the nuclear extracts from thymocytes was analyzed with NF-κB transcription factor colorimetric assay kit (Millipore). Nuclear extracts were incubated with biotinylated double-strand oligonucleotide probe containing the consensus sequence for NF-κB on a streptavidin-coated plate. Captured complexes, including active NF-κB protein, were incubated with the primary Abs for p50 and RelA and HRP-conjugated secondary Ab and tetramethylbenzidine substrate. The absorbance of the samples was measured with microplate reader at 450 nm.

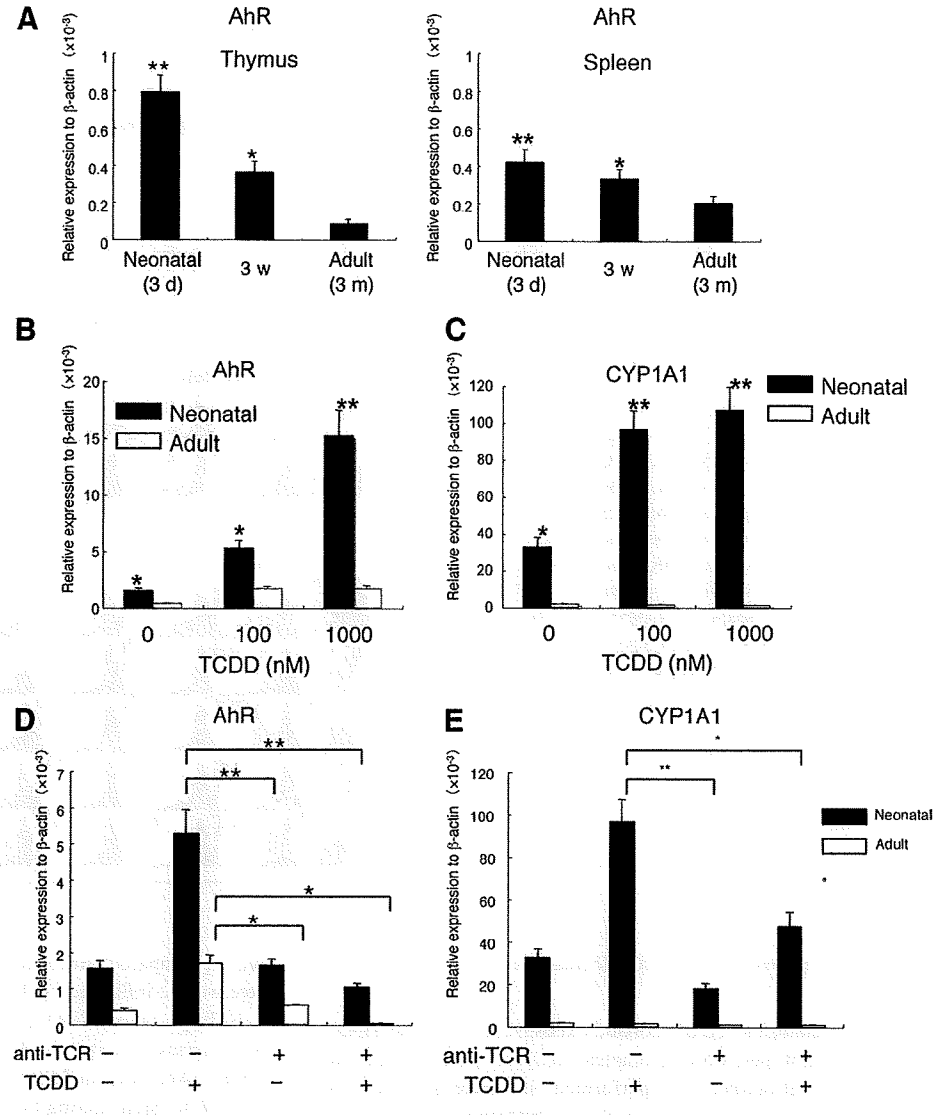

FIGURE 4. Cell signaling through AhR in thymus of NFS/*sld* mice. *A*, Expression of AhR mRNA of thymus and spleen from neonatal and adult NFS/*sld* mice was detected by quantitative RT-PCR. Relative expression to β-actin mRNA is indicated as mean ± SD of four mice in each group. *, $p < 0.05$; **, $p < 0.005$. w, Week. *B* and *C*, For 3 h in 24-well plate, 2×10^6 thymocytes of neonatal and adult NFS/*sld* mice were incubated with 0, 100, and 1000 nM TCDD. The mRNA expressions of AhR (*B*), and CYP1A1 (*C*) were analyzed by quantitative RT-PCR. *D* and *E*, The mRNA expressions of AhR (*D*) and CYP1A1 (*E*) in anti-TCR mAb-stimulated thymocytes from neonatal and adult mice with or without TCDD were detected by quantitative RT-PCR. Data are shown as mean ± SD of triplicate samples. *, $p < 0.05$; **, $p < 0.005$.

Statistical test

The Student *t* test was used for statistical analysis. Values of $p > 0.05$ were considered as significant.

Results

Induction of inflammatory lesions by neonatal administration of low-dose TCDD

To elucidate whether inflammatory lesions are induced by neonatal administration of low-dose TCDD into NFS/*sld* mice, i.p. injection of 0, 0.1, 1, and 10 ng/mouse TCDD was performed on day 0, 1, and 2 after birth. At 1, 2, and 6 mo of age, all the organs of treated mice were histopathologically analyzed. The inflammatory lesions in salivary glands of TCDD-injected mice, similar to those of thymectomized NFS/*sld* mice, were found whereas no lesion was observed in the salivary glands of vehicle-treated mice. The lesions of female mice were more severe than those of male mice (Fig. 1, *A–C*). Lymphocyte infiltration around ducts with destruction of acinar cells was observed in the TCDD-induced lesions (Fig. 1*A*). Severity of the inflammatory lesions was increased in a dose-dependent manner of TCDD (Fig. 1, *B* and *C*). In addition, more severe lesions developed with aging, and observed mainly in female mice (Fig. 1*C*). To characterize the infiltrating immune cells in the inflammatory lesions of salivary glands, the frozen sections were analyzed using the markers of T cells, B cells, and dendritic cells by immunofluorescence staining. $CD4^+$ T cells were mainly infiltrated in the inflammatory lesions of salivary glands from TCDD-treated mice, whereas a small population of $CD8^+$ T cells, B cells, and $CD11c^+$ dendritic cells were seen in the lesions (Fig. 1*D*).

In contrast, the inflammatory lesions of lung, liver, or kidney were also observed in the mice treated with TCDD (Fig. 1*E*). The incidence of the lesions is shown in Table I. At 6 mo of age, slight inflammatory lesions in the liver of 30–50% male mice by 0.1 or 1 ng of TCDD injection were observed. The inflammatory lesions of liver were found in 30–70% of male mice and ~50% of the female mice treated with 10 ng of TCDD at 6 mo of age. Also, the inflammatory lesions of lung with a small number of lymphocyte infiltrates around bronchus or blood vessels were observed in both 100% female and male mice treated with 10 ng of TCDD at 6 mo of age. In addition, the slight inflammation in the kidney from 100% male mice treated with 10 ng of TCDD was observed at 6 mo of age. As for female mice, the renal lesions were found in ~50% of the mice treated with 10 ng of TCDD at 6 mo of age. Induction of inflammatory lesions by TCDD might be dependent on the sex or the sensitivity of each organ, although its precise mechanism is unclear.

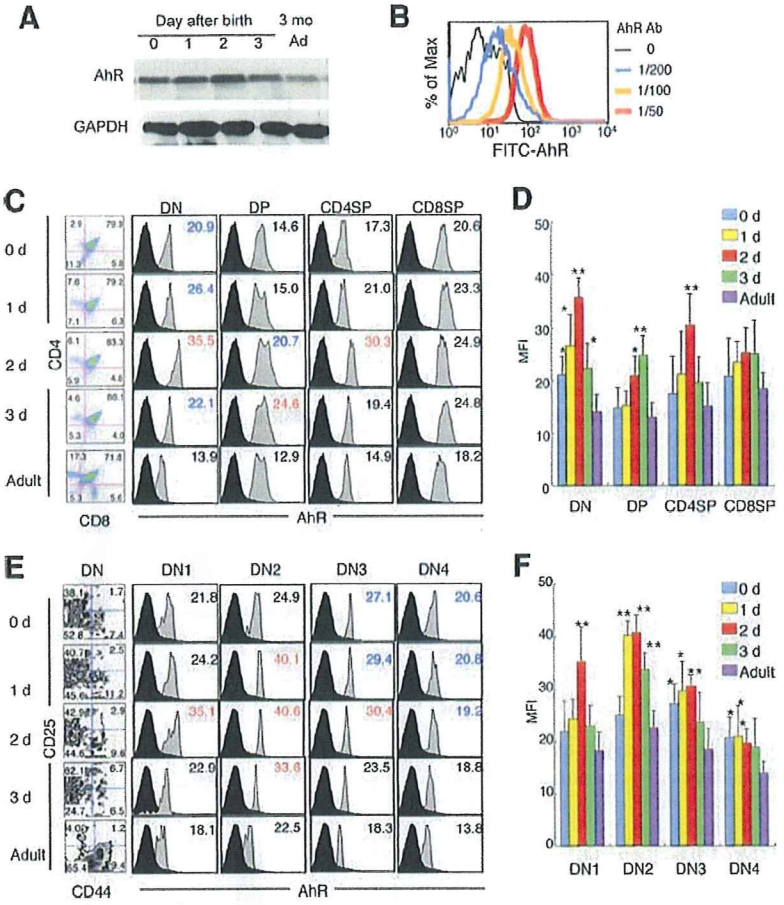

FIGURE 5. Expression of AhR in neonatal thymus. *A*, AhR protein of neonatal thymus from NFS/*sld* mice was detected by Western blotting. Result was representative of two independent experiments. GAPDH expression was used for loading control. *B*, Flow cytometric analysis of intracellular AhR expression. Thymocytes from B6 (3 mo) mice were stained with PE-Cy5.5-CD4 and PE-CD8 mAbs, fixed, washed in perm buffer, and then stained with rabbit anti-AhR Ab and FITC-conjugated anti-rabbit IgG as the second Ab. Diluted anti-AhR Ab (×200, ×100, and ×50) was used for staining. *C* and *D*, Thymocytes from neonatal (days 0, 1, 2, and 3 after birth) and adult (12 wk of age) NFS/*sld* mice were stained with PE-Cy5.5-CD4, PE-CD8, allophycocyanin-CD25, and PE-Cy7-CD44 mAbs, fixed, washed in permeabilization buffer, and then stained with rabbit anti-AhR Ab and FITC-conjugated anti-rabbit IgG as the second Ab. Intracellular AhR expressions of DN, DP, CD4SP, and CD8SP cells in neonatal and adult thymus. Figures are representative of three to four samples. Data are shown as mean ± SD of three to four samples. *E* and *F*, Intracellular AhR expression of DN cells in thymus. Data are shown as mean ± SD of mean fluorescence intensity (MFI) of three to four samples. Colored (blue or red) MFI was indicated in the figure as significantly increased. *, $p < 0.05$; **, $p < 0.005$.

Influence of in vivo low-dose TCDD injection on T cell phenotypes

To examine the influence of neonatal exposure to low-dose TCDD on T cell phenotypes, flow cytometric analysis of the expressions of surface T cell markers was performed on female mice at 6 mo of age (Fig. 2). There was no significant difference in the expression profile of CD4 and CD8 on the spleen cells by treatment of TCDD (Fig. 2*A*). A significantly increased population of memory phenotype, $CD44^{high}CD4^+$ T cell, was observed in the female mice treated with TCDD (Fig. 2*B*). As for thymic maturation, the $CD4^-CD8^-$ double-negative (DN) cells were considerably increased by treatment of 10 ng of TCDD while double-positive (DP) cells significantly decreased by 10 ng of TCDD injection. By contrast, both CD4 single-positive (SP) and CD8SP cells were significantly increased by TCDD injection (Fig. 2, *C* and *D*). Furthermore, when the increased DN cells were analyzed using differentiation markers such as CD25 and CD44, $CD44^+CD25^-$ (DN1) and $CD44^-CD25^-$ (DN4) cells were significantly reduced by in vivo treatment of 10 ng of TCDD, but significantly increased populations of $CD44^+CD25^+$ (DN2) and $CD44^-CD25^+$ (DN3) cells were observed (Fig. 2, *E* and *F*). These results suggested that neonatal exposure to TCDD might influence on thymic differentiation including negative or positive selection of T cells.

The influence of low-dose TCDD on peripheral T cell functions

To know the effect of TCDD on T cell functions in the periphery, cytokine secretions from splenic T cells activated by plate-coated anti-CD3 mAb were analyzed using the culture supernatants by ELISA. T_H1 cytokine production, including IL-2 and IFN-γ from activated T cells of TCDD-treated mice, was significantly increased compared with that of control mice (Fig. 3*A*). By contrast, there was no influence on T_H2 cytokine secretion such as IL-4 and IL-10 by in vivo TCDD injection (Fig. 3*A*). Moreover, proliferative response of splenic T cells stimulated with anti-CD3 and CD28 mAbs was analyzed using CFSE dilutions during 3 days. The cell divisions during the late stage were significantly enhanced by in vivo TCDD injection compared with those of control mice (Fig. 3*B*). In contrast, there was no difference in $Foxp3^+CD25^+CD4^+$ T cells, classical Treg cells, by neonatal TCDD exposure (Fig. 3*C*). It has been known that T-bet for T_H1 and GATA-3 for T_H2 are prime candidates for key transcription factors of each cytokine production of T_H cells (35). T-bet mRNA expression of purified T cells from spleen in TCDD-treated mice was higher than that in control mice. However, there was no change of the GATA-3 mRNA expression by TCDD injection (Fig. 3*D*). In addition, to examine the role of IL-17 in the pathogenesis for TCDD-induced autoimmunity, no change was observed in IL-17 production from anti-CD3 mAb-stimulated T cells of TCDD-treated mice (Fig. 3*E*). These findings show that the neonatal exposure to low-dose TCDD influences on T cell activation or proliferation through enhanced secretion of T_H1 cytokines in the periphery.

Direct influences of TCDD on neonatal thymus

When adult NFS/*sld* mice at 2 mo of age were injected with low-dose TCDD, no inflammatory lesion in any organ was observed until 6 mo of age (our unpublished data). Neonatal exposure to low-dose TCDD may affect the induction of inflammatory lesions in salivary glands resembling the SS model. To evaluate whether

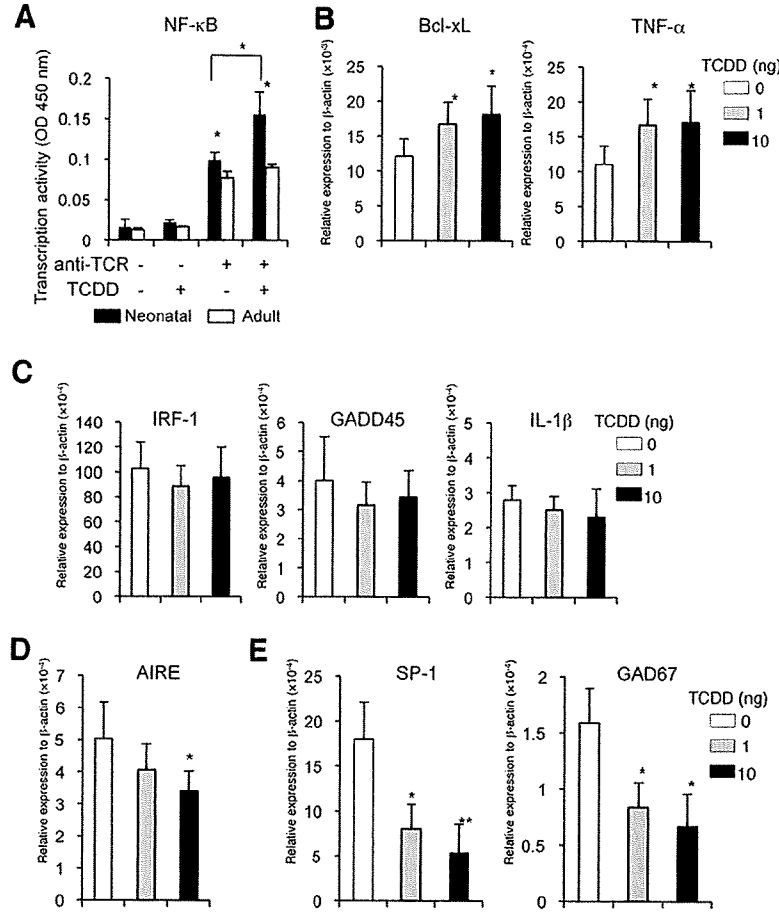

FIGURE 6. Influence of TCDD on central tolerance in thymus. *A*, Transcription activity of NF-κB in thymocytes stimulated with anti-TCR mAb in the presence or absence of TCDD was evaluated. Results are shown as mean ± SD of three samples. *, $p < 0.05$. *B* and *C*, In vivo effect of TCDD on target genes of NF-κB was evaluated to detect the mRNA expressions. The mRNA expressions of NF-κB-regulated genes in thymus tissues from TCDD-treated mice were analyzed by real time-PCR. Results are shown as mean ± SD of four to six mice per each group. *, $p < 0.05$. *D*, AIRE mRNA expression of thymus from TCDD-treated mice. *E*, The mRNA expressions of salivary protein-1 and GAD67 in thymus from TCDD-treated mice. The expressions of thymus from TCDD-treated mice were detected by real-time PCR. *, $p < 0.05$; **, $p < 0.005$.

the exposure to TCDD has much more influence on neonatal thymus compared with adult thymus, the expression of AhR was analyzed by quantitative RT-PCR. Interestingly, in contrast to adult thymus, the expression of AhR mRNA of neonatal thymus from NFS/*sld* mice was much higher (8- to 9-fold) (Fig. 4*A*). The expression was reduced with aging (~3 mo of age). The expression of AhR mRNA in neonatal spleen was higher (2-fold) than that in adult spleen (Fig. 4*A*). Next, to clarify the direct effects of TCDD on thymocytes, neonatal and adult thymocytes were incubated with 0, 100, and 1000 nM TCDD for 3 h to analyze AhR expression. More increased expression of AhR in neonatal thymocytes was observed by TCDD stimulation compared with that in adult thymocytes (Fig. 4*B*). In addition, mRNA expression of CYP1A1, one of target genes for TCDD/AhR/XRE (36), in neonatal thymocytes was much enhanced by TCDD incubation, whereas there was no change in mRNA expression of CYP1A1 in adult thymocytes by TCDD stimulation (Fig. 4*C*). In contrast, there were no significant changes in mRNA expressions of AhR and CYP1A1 of the spleen cells in the response to TCDD between neonatal and adult mice (data not shown). To understand association between TCR and TCDD signaling in thymocytes of neonatal and adult NFS/*sld* mice, plate-coated anti-TCRβ mAb was used for the stimulation of thymocytes with or without TCDD. Up-regulated mRNA expression of AhR by TCDD in both neonatal and adult thymocytes was clearly reduced by stimulation of anti-TCRβ mAb (Fig. 4*D*). In addition, TCDD-induced CYP1A1 mRNA expression in neonatal thymocytes was reduced to the level of non-stimulation by anti-TCRβ mAb (Fig. 4*E*). These findings suggest that neonatal thymocytes may be sensitive to TCDD through highly expressed AhR in NFS/*sld* mice, and that neonatal injection of TCDD might influence thymic differentiation to induce breakdown of tolerance.

Expression of AhR in neonatal thymus

To confirm the higher expression of AhR as a protein in neonatal thymus tissues of NFS/*sld* mice, Western blot analysis was performed. The highest expression of AhR was observed on day 2 after birth, and the expression on day 3 was relatively decreased. The expression in adult (3 mo of age) was lower than that of neonatal thymus (Fig. 5*A*). Next, we tried to detect the intracellular AhR expression in subpopulation of thymocytes by flow cytometric analysis. Flow cytometric analysis showed that most thymocytes clearly expressed AhR in adult (3 mo of age) C57BL/6 mice, and the fluorescence intensity of AhR expression was increased depending on the dose of anti-AhR Ab (Fig. 5*B*). When compared, the AhR expressions at each stage including DN, DP, CD4SP, and CD8SP cells in neonatal thymus of NFS/*sld* mice from day 0 to day 3 after birth with those in adult thymus (3 mo), a significantly increased AhR expression of neonatal (days 0, 1, 2, and 3) DN T cells was observed than that of adult DN cells. In particular, much more AhR expression of DN cells on day 2 was detected during neonatal stage. AhR expression of DP T cells on days 2 and 3 was significantly higher than that of adult DP cells. In contrast, although AhR expression of CD4SP cells on day 2 was significantly higher than that of adult CD4SP cells, there was no change in the expression of AhR of CD8SP cells between neonatal and adult thymus (Fig. 5, *C* and *D*). Furthermore, when the AhR expression of each differentiation stage of DN such as $CD44^+CD25^-$ (DN1), $CD44^+CD25^+$ (DN2), $CD44^-CD25^+$ (DN3), and $CD44^-CD25^-$

(DN4) cells was analyzed, AhR expressions of DN1 cells on day 2, DN2 cells on days 1, 2, and 3, DN3 cells on days 0, 1, and 2, and DN4 cells on days 0, 1, and 2 were significantly higher than those of adult DN cells (Fig. 5, *E* and *F*). Among them, the expressions of neonatal DN2 and DN3 cells were more intensive compared with those of adult thymocytes. In contrast, there was no difference in AhR expression at each stage between neonatal and adult thymocytes from normal B6 mice (data not shown). These findings suggest that AhR expression may be related with development and differentiation of T cells in neonatal thymus of NFS/*sld* mice, and that sensitivity of TCDD in neonates can be explained by the development of autoimmunity through AhR expression.

The influence of exposure to low-dose TCDD on central tolerance

Because higher AhR expression of T cells in neonatal thymus of NFS/*sld* mice was observed (Fig. 5), the cell signal pathway to regulate central tolerance in thymus via TCDD/AhR was analyzed. We focused on NF-κB, one of the responsive factors for TCDD/AhR/XRE signaling (37), which is known to be a key transcription factor for regulation of T cell differentiation, development, and activation (38). When the transcriptional activity of NF-κB in between neonatal and adult thymocytes stimulated with anti-TCR mAb in the presence of TCDD was compared, the neonatal activity was significantly increased relative to that of adult thymocytes (Fig. 6*A*). Also, the NF-κB activity of neonatal thymocytes stimulated with anti-TCR mAb was largely enhanced by the addition of TCDD, whereas the increased activity of adult thymocytes was not observed (Fig. 6*A*). Next, to understand the in vivo cell signaling through NF-κB and TCDD/AhR in thymus, the mRNA levels of NF-κB target genes were analyzed by real-time PCR using the thymus tissues from neonatal TCDD-treated mice. Among them, Bcl-xL and TNF-α mRNAs in thymus tissues from TCDD-treated mice were significantly increased in the dose-dependent manner compared with control mice (Fig. 6*B*). There were no changes to the mRNA expressions of IRF-1, GADD45, IL-1β (Fig. 6*C*), IL-6, inducible NO synthase, and Fas ligand (data not shown) which are target genes of NF-κB for controlling T cell signal.

In contrast, AIRE, an essential transcription factor for the expression of tissue-specific autoantigen in thymic epithelial cells (TECs), is well known to play a key role in T cell differentiation and development related with autoimmunity (39). When AIRE mRNA level in thymus tissues, including TECs from neonatal TCDD-treated NFS/*sld* mice, was analyzed, the expression in 10 ng of TCDD-treated mice was significantly decreased compared with that in control mice (Fig. 6*D*). Moreover, salivary protein-1 and GAD67 are known to be representative for the tissue-specific Ag in salivary gland and pancreas respectively (40). Interestingly, both salivary protein-1 and GAD67 mRNA expressions of the thymus tissues from neonatal TCDD-treated NFS/*sld* mice were significantly reduced relative to those from control mice (Fig. 6*E*). These findings show that neonatal exposure to low-dose TCDD in NFS/*sld* mice might influence the impairment of central tolerance in thymus, resulting in the induction of autoimmune disease.

The influences of low-dose TCDD exposure on B cells

The effects of neonatal exposure to low-dose TCDD on B cell phenotype and function were analyzed (Fig. 7). There was no difference in the number of $B220^+$ B cells from spleen between TCDD-treated and control mice (Fig. 7*A*). Furthermore, no change was observed in the proliferative response of splenic B cells to LPS from TCDD-treated mice compared with that from control mice (Fig. 7*B*). The serum titers of autoantibodies that are associated with SS, including anti-SSA/Ro, anti-SSB/La, and anti-ssDNA, were examined (17, 18). In this study, serum titers of anti-SSA/Ro and anti-SSB/La autoantibodies were significantly increased in TCDD-treated mice at 6 mo of age compared with those in control mice (Fig. 7*C*). It has been reported that thymectomized NFS/*sld* mice and human SS patients have high titers of serum autoantibody against α-fodrin (20, 34). The higher titers of anti-α-fodrin autoantibody in the sera from TCDD-treated mice were also detected from control mice at 6 mo of age (Fig. 7*D*). No significant change for anti-ssDNA was observed between TCDD-treated and control mice (data not shown). In addition, when the ratio of IgG2a and IgG1 that is associated with T_H1 and T_H2 or cellular and humoral immune responses was analyzed using sera from TCDD-injected mice, the ratio from TCDD-injected mice was significantly higher than that from control mice at 6 mo of age (Fig. 7*E*).

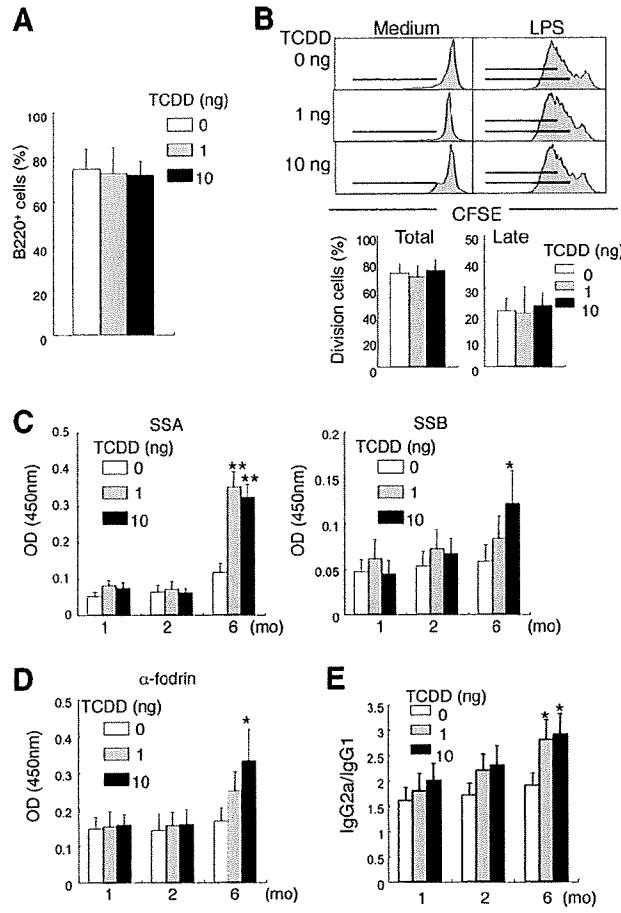

FIGURE 7. Influence on B cell functions by neonatal exposure to low-dose TCDD. *A*, $B220^+$ B cells in spleen from TCDD-treated mice at 6 mo of age were detected by flow cytometric analysis. Results are shown as mean ± SD of five to seven mice in each group. *B*, Proliferative response of splenic B cells stimulated with LPS was evaluated with CFSE dilutions during 72 h. Figures are representative of five to seven mice in each group. *C* and *D*, Serum titers of autoantibodies, including anti-SSA/Ro, anti-SSB/Lo, and anti-α-fodrin from female TCDD-treated mice from 1 to 6 mo of age were measured by ELISA. Results are shown as mean ± SD of five to seven mice in each group. *E*, Ratio of IgG2a/IgG1 in sera from TCDD-injected mice. Serum titer of IgG2a and IgG1 from TCDD-injected NFS/*sld* mice was measured by ELISA. Data are shown as mean ± SD of the ratio from five to seven mice. *, $p < 0.05$; **, $p < 0.005$.

Discussion

TCDD is a widespread environmental contaminant that influences several basic homeostatic control mechanisms in the body via AhR (3). T cells are a possible direct target for TCDD, as evidenced by the presence of the AhR in T cells, and inhibition of T cell growth by the expression of a constitutively active AhR mutant in AhR-null Jurkat T cells or following TCDD treatment (1, 41). It has been demonstrated that expression of AhR in both $CD4^+$ and $CD8^+$ T cells is required for a full suppression of an allospecific CTL response by TCDD, indicating a direct role for AhR in these TCDD-induced immunosuppressive effects (1, 42). However, the relationship between in vivo TCDD exposure and breakdown in T cell tolerance has not been well defined.

In this study, we demonstrated that neonatal exposure to low-dose TCDD could induce autoimmunity in the salivary glands using a NFS/*sld* strain associated with disease-susceptible autoantibody production, such as anti-SSA/La, anti-SSB/Ro, and anti-α-fodrin Abs. It has been reported that TCDD causes extensive damage to the thymus to suppress T cell-dependent immune responses in vivo, including delayed-type and contact hypersensitivity responses and the generation of CTL (4, 43, 44). By contrast, neonatal exposure to TCDD had little influence on thymic atrophy in our experiment in which low-dose (0.0486 ± 0.0088 to 8.37 ± 0.7 μg/kg) TCDD was administered into neonatal mice on days 0, 1, and 2 (body weight: 1.2 ± 0.1 to 2.1 ± 0.35 g) after birth. The dosage of TCDD was considerably lower than that in the experiments in which thymic atrophy or apoptosis was induced by in vivo exposure to TCDD (30–50 μg/kg) (31, 32). For instance, it was reported that 60% apoptotic cells of thymus were observed in normal mice injected with 50 μg/kg TCDD, whereas 20–30% apoptotic cells of thymus were observed in vehicle-injected mice. In addition, although the loss of mitochondrial membrane potential related to apoptosis of thymocytes was not detected in ~10 μg/kg TCDD-treated mice, the loss was observed in 10–50 μg/kg TCDD-treated mice (31). Thus, the exposure to low dosage under 10 μg/kg TCDD may have an influence on neonatal thymic differentiation or selection in NFS/*sld* mice, but not atrophy or apoptosis, to induce autoimmune disease as the late effect. Moreover, T cell proliferation by anti-CD3 and -CD28 mAbs and Th1-type cytokine production, such as IL-2 and IFN-γ from splenic $CD4^+$ T cells, were significantly more enhanced by neonatal TCDD treatment than those in control mice. These findings were consistent with the reports that TCDD enhances proliferation and cytokine production of mitogen- or Ag-stimulated T cells or T cell clones (1, 8). Because there were alterations in the percentage and number of DN cells in TCDD-treated mice, we analyzed this population using CD44 and CD25 markers. After TCDD treatment in this set, there was a decrease in the percentage of $CD44^+CD25^-$ cells (DN1) and $CD44^-CD25^-$ cells (DN4), and a relative increase in the percentage of $CD44^+CD25^+$ cells (DN2) and $CD44^-CD25^+$ cells (DN3). Analysis of the actual numbers of cells in each population compared with controls suggested that thymic maturation or negative selection at DN2 or DN3 might be affected by neonatal exposure to the low-dose TCDD. These results suggest that TCDD is interfering with the development and/or the proliferation of DN cells. Furthermore, the early stage of DN and the late stage into CD4SP or CD8SP in the thymic differentiation were disturbed by low-dose TCDD treatment, indicating that the immunotoxicity of TCDD on neonatal thymus might lead to the development of T cell-dependent autoimmunity. The inflammatory lesions were observed in the organs other than salivary gland including kidney, lung, and liver in TCDD-treated mice. Although the inflammatory lesions in liver, lung, and kidney from female mice treated with 10 ng of TCDD at 2 mo of age were observed, the severity of extraglandular lesions was lower than that of salivary gland, and the onset was later compared with that in salivary gland. Most of the extraglandular lesions of both female and male mice were developed with aging. We have previously demonstrated that the extraglandular lesion such as autoimmune arthritis in 3d-Tx NFS/*sld* mice was observed with aging (45, 46). Therefore, it is possible that TCDD may enhance any age-related reaction in the organs to induce autoimmunity.

In this study, there were no changes in the B cell number and proliferation in spleen from low-dose TCDD-treated mice, although the suppressive effect of the T cell-dependent Ab response to sheep RBC was reported in C57BL/6 mice injected with TCDD (47). In addition, TCDD selectively inhibited terminal B cell differentiation into plasma cells in response to trinitrophenol-LPS without altering early events in B cell activation or proliferation (48). By contrast, in our study significantly increased autoantibody productions such as anti-SSA/La, anti-SSB/Ro, and anti-α-fodrin were observed by neonatal exposure to low-dose TCDD. Although it is still unclear whether the direct or indirect effect of TCDD on B cells influences autoantibody production, this new finding may be a key to understand the association of TCDD immunotoxicity with the development of autoimmunity.

AhR is a cytoplasmic receptor protein and has been described as a ligand-activated transcription factor that mediates induction of xenobiotic metabolizing enzymes (27, 28, 49). Upon ligand binding, the AhR translocates into the nucleus and dimerizes with ARNT. The AhR/ARNT complex binds to specific gene promoter elements (50). In this study, significantly increased expressions of AhR mRNA and protein in neonatal thymus were observed compared with those in adult thymus. This suggests that neonatal exposure to low-dose TCDD may effect thymic differentiation and/or maturation through AhR by disrupting the T cell tolerance more intensively than those in adult thymus. If negative or positive selection in the neonatal thymus is disrupted by low-dose TCDD exposure, autoreactive T cells may be released to the periphery and expand in response to any autoantigen leading to induce autoimmunity. Increased expression of AhR mRNA and the disrupted thymic differentiation in the neonatal thymus by low-dose TCDD exposure may support this hypothesis.

CYP1A1 is known to have pivotal roles in cell growth and apoptosis (51, 52). In the present study, CYP1A1 mRNA of neonatal thymocytes was readily up-regulated by TCDD, whereas the expression of adult thymocytes was constant in the response to TCDD. Neonatal exposure to low-dose TCDD may influence proliferation, differentiation, or apoptosis of thymocytes through CYP1A1 at early stages, such as DN. Namely, it is possible that negative selection leading cell apoptosis at DN3 might be disturbed by neonatal exposure to TCDD. As a result, autoreactive T cells leaking from thymic selection might survive and proliferate in response to any autoantigen in the periphery, leading to the induction of autoimmune lesions. The activation of AhR by TCDD results in an increased binding activity to NF-κB subunit RelB of AhR itself to form AhR/RelB complex, which was associated with an increased mRNA level of multiple inflammatory genes (53). Overexpression of AhR and RelB led to an increased level of CCL1 and IRF-3 in control as well as TCDD-stimulated cells supporting the role of RelB and AhR for the transcriptional regulation of these genes (54). In the present study, TCDD enhanced TCR-mediated classical NF-κB activation of neonatal thymocytes from NFS/*sld* mice more than adult thymocytes. In addition, some NF-κB-target genes such as Bcl-x_L and TNF-α in thymus were up-regulated by in vivo TCDD injection. Our data demonstrate that

TCDD/AhR signal may influence the differentiation or development of T cells in the neonatal thymus associated with autoimmunity. However, the precise mechanism of how the NF-κB activation, including classical and nonclassical pathway, interacts with TCDD/AhR signal is still unclear.

It has been well known that autoimmune lesions of multiple organs such as lacrimal glands, salivary glands, pancreas, and liver are observed in AIRE gene-deficient mice (39). AIRE was reported to play a pivotal role in the expression of tissue-specific autoantigens such as salivary protein-1, GAD67, insulin, or other self-proteins in the TECs that express the MHC class II on the cell surface and function as APCs to immature T cells for the immunological selection of central tolerance in the thymus (55). In this study, mRNA expressions of AIRE and tissue-specific autoantigens such as salivary protein-1 and GAD67 in the thymus were reduced by the in vivo neonatal exposure to low-dose TCDD in NFS/*sld* mice. The finding indicated that TCDD might influence the selection of autoreactive T cells in the thymus through AIRE. There may be any complex molecular mechanisms related to the avidity of TCR, haplotype of MHC class II, Ag-specificity, T cell apoptosis, interaction with TEC, or TCDD signal.

The AhR has been shown to mediate various immunotoxic responses induced by environmental pollutants like TCDD (56). Although our results show that activation of the AhR by TCDD effects T cell development, the receptor does not seem to play a key role in the establishment of a normal T cell compartment. The AhR has been shown to play important roles in regulating the expression of several cytokines. For example, exposure of rats to TCDD led to up-regulation of IL-1β and TNF-α in the liver (57, 58). Interestingly, although TCDD suppressed the production of IFN-γ by mediastinal lymph node cells, there was a 10-fold increase in the IFN-γ level in the lungs of TCDD-treated mice (59). Autoimmune disease is caused by heterogeneous etiology, involving interplay between predisposing genes and triggering environmental factors. Although a lot of studies have demonstrated the immunotoxicity of TCDD, this study is the first to induce autoimmunity by neonatal low-dose TCDD treatment. Recently it has been reported that AhR links T_H17 cell-mediated experimental autoimmune encephalomyelitis to environmental toxins through altering the differentiation of Treg cells (60, 61). The low-dose TCDD exposure in our model had little influence on the number of Treg cells in spleen and the function of T_H17 cells, such as IL-17 production from T cells. The action of TCDD via AhR may influence peripheral tolerance related to autoimmunity besides central tolerance in thymus.

Taken together, our new findings may explain the risk for autoimmunity caused by the late effect of early exposure to environmental pollution, including TCDD. And as shown here, our model would help to understand the multifactorial nature of autoimmune disease.

Acknowledgments

We thank Ai Nagaoka, Noriko Kino, Risa Okada, Ritsuko Oura, and Satoko Yoshida for technical assistance.

Disclosures

The authors have no financial conflict of interest.

References

1. Kerkvliet, N. I. 2001. Recent advances in understanding the mechanisms of TCDD immunotoxicity. *Int. Immunopharmacol.* 2: 277–291.
2. Wormley, D. D., A. Ramesh, and D. B. Hood. 2004. Environmental contaminant-mixture effects on CNS development, plasticity, and behavior. *Toxicol. Appl. Pharmacol.* 197: 49–65.
3. Schecter, A., L. Birnbaum, J. J. Ryan, and J. D. Constable. 2006. Dioxins: an overview. *Environ. Res.* 101: 419–428.
4. Laiosa, M. D., A. Wyman, F. G. Murante, N. C. Fiore, J. E. Staples, T. A. Gasiewicz, and A. E. Silverstone. 2003. Cell proliferation arrest within intrathymic lymphocyte progenitor cells causes thymic atrophy mediated by the aryl hydrocarbon receptor. *J. Immunol.* 171: 4582–4591.
5. Gehrs, B. C., and R. J. Smialowicz. 1999. Persistent suppression of delayed-type hypersensitivity in adult F344 rats after perinatal exposure to 2,3,7,8-tetrachlorodibenzo-p-dioxin. *Toxicology* 134: 79–88.
6. Walker, D. B., W. C. Williams, C. B. Copeland, and R. J. Smialowicz. 2004. Persistent suppression of contact hypersensitivity, and altered T-cell parameters in F344 rats exposed perinatally to 2,3,7,8-tetrachlorodibenzo-*p*-dioxin (TCDD). *Toxicology* 197: 57–66.
7. Prell, R. A., E. Dearstyne, L. G. Steppan, A. T. Vella, and N. I. Kerkvliet. 2000. CTL hyporesponsiveness induced by 2,3,7,8-tetrachlorodibenzo-*p*-dioxin: role of cytokines and apoptosis. *Toxicol. Appl. Pharmacol.* 166: 214–221.
8. Prell, R. A., J. A. Oughton, and N. I. Kerkvliet. 1995. Effect of 2,3,7,8-tetrachlorodibenzo-*p*-dioxin on anti-CD3-induced changes in T-cell subsets and cytokine production. *Int. J. Immunopharmacol.* 17: 951–961.
9. Shepherd, D. M., E. A. Dearstyne, and N. I. Kerkvliet. 2000. The effects of TCDD on the activation of ovalbumin (OVA)-specific DO11.10 transgenic CD4(+) T cells in adoptively transferred mice. *Toxicol. Sci.* 56: 340–350.
10. Morris, D. L., J. G. Karras, and M. P. Holsapple. 1993. Direct effects of 2,3,7,8-tetrachlorodibenzo-p-dioxin (TCDD) on responses to lipopolysaccharide (LPS) by isolated murine B-cells. *Immunopharmacology* 26: 105–112.
11. Karras, J. G., and M. P. Holsapple. 1994. Inhibition of calcium-dependent B cell activation by 2,3,7,8-tetrachlorodibenzo-*p*-dioxin. *Toxicol. Appl. Pharmacol.* 125: 264–270.
12. Dooley, R. K., D. L. Morris, and M. P. Holsapple. 1990. Elucidation of cellular targets responsible for tetrachlorodibenzo-p-dioxin (TCDD)-induced suppression of antibody responses. II. The role of the T-lymphocyte. *Immunopharmacology* 19: 47–58.
13. Gotter, J., and B. Kyewski. 2004. Regulating self-tolerance by deregulating gene expression. *Curr. Opin. Immunol.* 16: 741–745.
14. Anderton, S., C. Burkhart, B. Metzler, and D. Wraith. 1999. Mechanisms of central and peripheral T-cell tolerance: lessons from experimental models of multiple sclerosis. *Immunol. Rev.* 169: 123–127.
15. Miller, J. F., and R. A. Flavell. 1994. T-cell tolerance and autoimmunity in transgenic models of central and peripheral tolerance. *Curr. Opin. Immunol.* 6: 892–899.
16. Kruize, A. A., R. J. Sweenk, and L. Kater. 1995. Diagnostic criteria and immunopathogenesis of Sjögren's syndrome: implications for therapy. *Immunol. Today* 16: 557–559.
17. Fox, R. I., M. Stern, and P. Michelson. 2000. Update in Sjögren syndrome. *Curr. Opin. Rheumatol.* 12: 391–398.
18. Fox, R. I. 2005. Sjögren's syndrome. *Lancet* 366: 321–331.
19. Haneji, N., H. Hamano, K. Yanagi, and Y. Hayashi. 1994. A new animal model for primary Sjögren's syndrome in NFS/*sld* mutant mice. *J. Immunol.* 153: 2769–2777.
20. Haneji, N., T. Nakamura, K. Takio, K. Yanagi, H. Higashiyama, I. Saito, S. Noji, H. Sugino, and Y. Hayashi. 1997. Identification of α-fodrin as a candidate autoantigen in primary Sjögren's syndrome. *Science* 275: 604–607.
21. Saegusa, K., N. Ishimaru, K. Yanagi, K. Mishima, R. Arakaki, T. Suda, I. Saito, and Y. Hayashi. 2002. Prevention and induction of autoimmune exocrinopathy is dependent on pathogenic autoantigen cleavage in murine Sjögren's syndrome. *J. Immunol.* 169: 1050–1057.
22. Suri-Payer, E., K. Wei, and K. Tung. 2001. The day-3 thymectomy model for induction of multiple organ-specific autoimmune diseases. *Curr. Protoc. Immunol.* 15: 15–16.
23. Kojima, A., Y. Tanaka-Kojima, T. Sakakura, and Y. Nishizuka. 1976. Spontaneous development of autoimmune thyroiditis in neonatally thymectomized mice. *Lab. Invest.* 34: 550–557.
24. Teague, P. O., E. J. Yunis, G. Rodey, A. J. Fish, O. Stutman, and R. A. Good. 1970. Autoimmune phenomena and renal disease in mice: role of thymectomy, aging, and involution of immunologic capacity. *Lab. Invest.* 22: 121–130.
25. Tung, K. S., S. Smith, P. Matzner, K. Kasai, J. Oliver, F. Feuchter, and R. E. Anderson. 1987. Murine autoimmune oophoritis, epididymoorchitis, and gastritis induced by day 3 thymectomy. *Am. J. Pathol.* 126: 303–314.
26. Safe, S. 2001. Molecular biology of the Ah receptor and its role in carcinogenesis. *Toxicol. Lett.* 120: 1–7.
27. Denison, M. S., and S. Heath-Pagliuso. 1998. The Ah receptor: a regulator of the biochemical and toxicological actions of structurally diverse chemicals. *Bull. Environ. Contam. Toxicol.* 61: 557–568.
28. Marlowe, J. L., and A. Puga. 2005. Aryl hydrocarbon receptor, cell cycle regulation, toxicity, and tumorigenesis. *J. Cell. Biochem.* 96: 1174–1184.
29. Nohara, K., H. Fujimaki, S. Tsukumo, K. Inouye, H. Sone, and C. Tohyama. 2002. Effects of 2,3,7,8-tetrachlorodibenzo-*p*-dioxin (TCDD) on T cell-derived cytokine production in ovalbumin (OVA)-immunized C57Bl/6 mice. *Toxicology* 172: 49–58.
30. Neff-LaFord, H. D., B. A. Vorderstrasse, and B. P. Lawrence. 2003. Fewer CTL, not enhanced NK cells, are sufficient for viral clearance from the lungs of immunocompromised mice. *Cell. Immunol.* 226: 54–64.
31. Tomita, S., H. B. Jiang, T. Ueno, S. Takagi, K. Tohi, S. Maekawa, A. Miyatake, A. Furukawa, F. J. Gonzalez, J. Takeda, T. Ichikawa, and Y. Takahama. 2003. T cell-specific disruption of arylhydrocarbon receptor nuclear translocator (Arnt) gene causes resistance to 2,3,7,8-tetrachlorodibenzo-*p*-dioxin-induced thymic involution. *J. Immunol.* 171: 4113–4120.
32. Camacho, I. A., N. Singh, V. L. Hegde, M. Nagarkatti, and P. S. Nagarkatti. 2005. Treatment of mice with 2,3,7,8-tetrachlorodibenzo-*p*-dioxin leads to aryl

hydrocarbon receptor-dependent nuclear translocation of NF-κB and expression of Fas ligand in thymic stromal cells and consequent apoptosis in T cells. *J. Immunol.* 175: 90–103.
33. White, S. C., and G. W. Casarett. 1974. Induction of experimental autoallergic sialadenitis. *J. Immunol.* 112: 178–185.
34. Kohashi, M., N. Ishimaru, R. Arakaki, and Y. Hayashi. 2008. Effective treatment with oral administration of rebamipide in a mouse model for Sjogren's syndrome. *Arthritis Rheum.* 58: 389–400.
35. Rengarajan, J., S. J. Szabo, and L. H. Glimcher. 2000. Treanscriptional regulation oh Th1/Th2 polarization. *Immunol. Today* 21: 479–783.
36. Riddick, D. S., Y. Huang, P. A. Harper, and A. B. Okey. 1994. 2,3,7,8-Tetrachlorodibenzo-*p*-dioxin versus 3-methylcholanthrene: comparative studies of Ah receptor binding, transformation, and induction of CYP1A1. *J. Biol. Chem.* 269: 12118–12128.
37. Singh, N. P., M. Nagarkatti, and P. S. Nagarkatti. 2007. Role of dioxin response element and nuclear factor-κB motifs in 2,3,7,8-tetrachlorodibenzo-*p*-dioxin-mediated regulation of Fas and Fas ligand expression. *Mol. Pharmacol.* 71: 145–157.
38. Bonizzi, G., and M. Karin. 2004. The two NF-κB activation pathways and their role in innate and adaptive immunity. *Trends Immmol.* 25: 280–288.
39. Anderson, M. S., E. S. Venanzi, L. Klein, Z. Chen, S. P. Berzins, S. J. Turley, H. von Boehmer, R. Bronson, A. Dierich, C. Benoist, and D. Mathis. 2002. Protection of an immunological self shadow within the thymus by the aire protein. *Science* 298: 1395–1401.
40. Kuroda, N., T. Mitani, N. Takeda, N. Ishimaru, R. Arakaki, Y. Hayashi, Y. Bando, K. Izumi, T. Takahashi, T. Nomura, et al. 2005. Development of autoimmunity against transcriptionally unrepressed target antigen in the thymus of Aire-deficient mice. *J. Immunol.* 174: 1862–1870.
41. Ito, T., S. Tsukumo, N. Suzuki, H. Motohashi, M. Yamamoto, Y. Fujii-Kuriyama, J. Mimura, T. M. Lin, R. E. Peterson, C. Tohyama, and K. Nohara. 2004. A constitutively active arylhydrocarbon receptor induces growth inhibition of Jurkat T cells through changes in the expression of genes related to apoptosis and cell cycle arrest. *J. Biol. Chem.* 279: 25204–25210.
42. Nagarkatti, P. S., G. D. Sweeney, J. Gauldie, and D. A. Clark. 1984. Sensitivity to suppression of cytotoxic T cell generation by 2,3,7,8-tetrachlorodibenzo-*p*-dioxin (TCDD) is dependent on the Ah genotype of the murine host. *Toxicol. Appl. Pharmacol.* 72: 169–176.
43. Nohara, K., X. Pan, S. Tsukumo, A. Hida, T. Ito, H. Nagai, K. Inouye, H. Motohashi, M. Yamamoto, Y. Fujii-Kuriyama, and C. Tohyama. 2005. Constitutively active aryl hydrocarbon receptor expressed specifically in T-lineage cells causes thymus involution and suppresses the immunization-induced increase in splenocytes. *J. Immunol.* 174: 2770–2777.
44. Staples, J. E., F. G. Murante, N. C. Fiore, T. A. Gasiewicz, and A. E. Silverstone. 1998. Thymic alterations induced by 2,3,7,8-tetrachlorodibenzo-*p*-dioxin are strictly dependent on aryl hydrocarbon receptor activation in hemopoietic cells. *J. Immunol.* 160: 3844–3854.
45. Ishimaru, N., T. Yoneda, K. Saegusa, K. Yanagi, N. Haneji, K. Moriyama, I. Saito, and Y. Hayashi. 2000. Severe destructive autoimmune lesions with aging in murine Sjögren's syndrome through Fas-mediated apoptosis. *Am. J. Pathol.* 156: 1557–1564.
46. Kobayashi, M., N. Yasui, N. Ishimaru, R. Arakaki, and Y. Hayashi. 2004. Development of autoimmune arthritis with aging via bystander T cell activation in the mouse model of Sjögren's syndrome. *Arthritis Rheum.* 50: 3974–3984.
47. Kerkvliet, N. I., and J. A. Brauner. 1987. Mechanisms of 1,2,3,4,6,7,8-heptachlorodibenzo-*p*-dioxin (HpCDD)-induced humoral immune suppression: evidence of primary defect in T-cell regulation. *Toxicol. Appl. Pharmacol.* 87: 47–58.
48. Luster, M. I., D. R. Germolec, G. Clark, G. Wiegand, and G. J. Rosenthal. 1998. Selective effects of 2,3,7,8-tetrachlorodibenzo-*p*-dioxin and corticosteroid on in vitro lymphocyte maturation. *J. Immunol.* 140: 928–935.
49. Schmidt, J. V., G. H. Su, J. K. Reddy, M. C. Simon, and C. A. Bradfield. 1996. Characterization of a murine Ahr null allele: involvement of the Ah receptor in hepatic growth and development. *Proc. Natl. Acad. Sci. USA* 93: 6731–6736.
50. Gu, Y. Z., J. B. Hogenesch, and C. A. Bradfield. 2000. The PAS superfamily: sensors of environmental and developmental signals. *Annu. Rev. Pharmacol. Toxicol.* 40: 519–561.
51. Umannova, L., J. Zatloukalova, M. Machala, P. Kremar, Z. Majkova, B. Hennig, A. Kozubik, and J. Vondracek. 2007. Tumor necrosis factor-α modulates effects of aryl hydrocarbon receptor ligands on cell proliferation and expression of cytochrome P450 enzymes in rat liver "stem-like" cells. *Toxicol. Sci.* 99: 79–89.
52. Hoagland, M. S., E. Hoagland, and H. I. Swanson. 2005. The p53 inhibitor pifithrin-α is a potent agonist of aryl hydrocarbon receptor. *J. Pharmacol. Exp. Ther.* 314: 603–610.
53. Vogel, C. F., E. Sciullo, W. Li, P. Wong, G. Lazennec, and F. Matsumura. 2007. RelB, a new partner of aryl hydrocarbon receptor-mediated transcription. *Mol. Endocrinol.* 21: 2941–2955.
54. Vogel, C. F., E. Sciullo, and F. Matsumura. 2007. Involvement of RelB in aryl hydrocarbon receptor-mediated induction of chemokines. *Biochem. Biophys. Res. Commun.* 363: 722–726.
55. Gillard, G. O., and A. G. Farr. 2005. Contrasting models of promiscuous gene expression by thymic epithelium. *J. Exp. Med.* 202: 15–19.
56. Mandal, P. K. 2005. Dioxin: a review of its environmental effects and its aryl hydrocarbon receptor biology. *J. Comp. Physiol.* 175: 221–230.
57. Fan, F., B. Yan, G. Wood, M. Viluksela, and K. K. Rozman. 1997. Cytokines (IL-1β and TNFα) in relation to biochemical and immunological effects of 2,3,7,8-tetrachlorodibenzo-*p*-dioxin (TCDD) in rats. *Toxicology* 116: 9–16.
58. Vogel, C., S. Donat, O. Döhr, L. Kremer, C. Esser, M. Roller, and J. Abel. 1997. Effect of subchronic 2,3,7,8-tetrachlorodibenzo-*p*-dioxin exposure on immune system and target gene responses in mice: calculation of benchmark doses for CYP1A1 and CYP1A2 related enzyme activities. *Arch. Toxicol.* 71: 372–382.
59. Warren, T. K., K. A. Mitchell, and B. P. Lawrence. 2000. Exposure to 2,3,7,8-tetrachlorodibenzo-*p*-dioxin (TCDD) suppresses the humoral and cell-mediated immune responses to influenza A virus without affecting cytolytic activity in the lung. *Toxicol. Sci.* 56: 114–123.
60. Veldhoen, M., K. Hirota, A. M. Westendorf, J. Buer, L. Dumoutier, J. C. Renauld, and B. Stockinger. 2008. The aryl hydrocarbon receptor links TH17-cell-mediated autoimmunity to environmental toxins. *Nature* 453: 106–110.
61. Quintana, F. J., A. S. Basso, A. H. Iglesias, T. Korn, M. F. Farez, E. Bettelli, M. Caccamo, M. Oukka, and H. L. Weiner. 2008. Control of Treg and TH17 cell differentiation by the aryl hydrocarbon receptor. *Nature* 453: 65–72.

The Journal of Toxicological Sciences (J. Toxicol. Sci.)
Vol.34, Special Issue II, SP199-SP200, 2009

Overview: "Children's Toxicology", a renovating study field of irreversible "early exposure-delayed effects"

Jun Kanno

Division of Cellular and Molecular Toxicology, Biological Safety Research Center, National Institute of Health Sciences, 1-18-1 Kamiyoga, Setagaya-ku, Tokyo 158-8501, Japan

(Received February 17, 2009)

ABSTRACT — "Children are not small adults". This is a well-known phrase, especially in the clinics for diagnosis, efficacy of treatment, side effect, and prognosis. However, in the field of toxicology, this issue has long been a challenge. The knowledge has been limited to the differences in metabolism and other physiological factors. Currently available test guidelines for fetuses and immature animals are teratogenicity and reproductive toxicity studies. These tests look for straight-forward (essentially macroscopic) outcomes established within a rather short period of exposure to the test substances. However, recent advances in molecular toxicology allow combination of *in vitro* and *in vivo* studies at molecular levels. The target molecules and receptors can be identified in quantitative fashion and at the fine structure levels around and below the resolution of normal light microscopy. Such expansion of the knowledge lead us to consider a rather new category of "receptor mediated toxicity" or "signal toxicity". Such non-organic insults would merely induce transient effects on adults. However, there are growing evidences that such slight insults on the developing and maturating organisms can leave irreversible effects that become overt in adulthood. As an overview, toxicology has entered a new phase where children's toxicology becomes a renovating study field of the irreversible "early exposure-delayed effects".

Key words: Children's toxicology, Receptor-mediated toxicity, Signal toxicity, Early exposure-delayed effect

INTRODUCTION

Toxicology is a study to analyze interaction between living organisms and xenobiotics, and its final goal is to secure the safety of humans and environment in modern life where various products and technologies are used. Up to now, the majority of toxicological tests to evaluate the toxicity of a particular substance are utilizing experimental animals as a surrogate of humans. The results obtained from such animal tests are extrapolated to humans for the settlement of various kinds of regulation on the test substances, i.e. food additives, pesticides, industrial chemicals, medicines, etc. In cases of pharmaceutical products, clinical trials (human tests) are available. However, these are rather exceptional occasions for toxicology as a whole. It would be very difficult for non-pharmaceutical objects to test on humans, and even for pharmaceuticals, human trial for children including fetuses have many difficulties.

Current toxicological testing protocols are based on an assumption that both experimental animals and humans share common basic structure of the body and thus similar biological reaction. Most of those toxicological studies are based on "diagnosis" of the symptoms of experimental animals in a similar fashion to give a diagnosis to human patients. Because the fine structure and function of the bodies are still unknown, both humans and animal bodies are "black boxes" responding to the test substances by showing various symptoms. Usually, the "no observed adverse effect level" (NOAEL) or "no observed effect level" (NOEL) is given by such tests. Since the basic nature of species differences and individual differences are not known, a number called "safety factor" was invented to extrapolate animal NOAEL/NOEL data to humans (Benford, 2000). Normally, a factor of 10 for the species and another 10 for individual differences, thus 100 as a whole, is used to set lower NOAEL/NOEL levels for humans. This approach has been working well for the majority of test substances. Not surprisingly, however, there are some exceptions. Thalidomide is a best-known example (Newman, 1985). Phocomelia, a spectrum of malformation of limbs, was induced in offspring of tha-

Correspondence: Jun Kanno (E-mail: kanno@nihs.go.jp)

lidomide-treated pregnant women, but not observed in offspring of mice and rats. Therefore, more precise toxicity evaluation/prediction is obviously needed for safer assessment. An approach that enables us to point out molecular mechanisms of toxicity would be essential for such needs and to better understand the species-specific responses.

DISCUSSION

To modernize the toxicology and improve the accuracy of safety assessments, we are attempting to describe and understand the organism-xenobiotics interaction at the molecular levels. Different for other exploratory studies, a major prerequisite is that the Toxicology must be prepared for any unexpected or unpredictable responses. Thus, the approach must be comprehensive. Consequently, we adopted a whole-genome cDNA microarray system for a comprehensive monitoring of the transcriptome, and launched the Percellome Toxicogenomics Project, of which the ultimate goal is to illustrate out the whole regulatory pathways induced by xenobiotics in the experimental animals, mainly mice, including embryo (Kanno *et al.*, 2006).

On top of that, there is an important factor of toxicology, that it the "time frame" such as acute, chronic and delayed toxicity. Among them, researches for the assessment of delayed toxicity targeted for children (including fetus and infants) is becoming very important. It is very likely that the children have a chance to be exposed in daily life to a series of substances which can be a cause of delayed toxicity, especially, of the highly evolved systems, that is endocrine, immune and central nervous system. Such chemical substances can affect the developing systems at a dosage lower than the dosage that induces overt cytocidal changes that would link to immediate appearance of symptoms. For example, our recent experience on the perinatal exposure study (Tanemura *et al.*, 2009) which resulted in the emergence of delayed effects on neurobehavioral endpoints can be explained by a metaphor. That is, "No one turns on power when building a computer, but the living brains are built under the "power-on" situation". It is very likely that the developing brain needs proper or normal signals to build up its fine structures and functional networks (Cohen-Cory, 2002). At this stage, if the signals are disrupted by exogenous insults, it may result in malformation of the fine structure of the brain system. In this case, it is not necessary to directly kill the nerve cells during exposure. The malformation of fine structure/functional network will become symptomatic when the animals grow up to adults. On the other hand, most of those insults to adults would end up in reversible and transient changes.

Such delayed toxicity cannot be readily detected by currently available functional observational battery-(FOB-) based neuronal test system. Our new findings fall into the category of "early exposure- delayed effect". As mentioned above, nervous systems of developing organisms are susceptible to signal disruption which could lead to the delayed neurobehavioral anomaly. Toxicology is asked to prepare to respond to such new types of toxicity or "signal toxicity" with a consideration on the mechanisms which could explain the severity and irreversibility specific to children.

In conclusion, the 35th Annual Meeting of the Japanese Society of Toxicology had raised "Children's Toxicology" as one of its main Themes, and organized Special lectures, five Symposiums and two Workshops on Children's Toxicology of various targets and pending problems, which includes central nervous system, immune system, and endocrine system as targets, as well as problems in pharmacology i.e. issues on children's preclinical and clinical trials and on the off-label use of drugs. This special issue of the Journal of Toxicological Sciences gathers the peer-reviewed papers presented by the authors who participated in the lectures/symposiums/workshops on Children's Toxicology at the meeting.

REFERENCES

Benford, D. (2000): The Acceptable Daily Intake: A food for ensuring food safety. ILSI Europe Concise Monograph series. Brussels, Belgium.

Cohen-Cory, S. (2002): The developing synapse: construction and modulation of synaptic structures and circuits. Science, **298**, 770-776.

Kanno, J., Aisaki, K., Igarashi, K., Nakatsu, N., Ono, A., Kodama, Y. and Nagao, T. (2006): "Per cell" normalization method for mRNA measurement by quantitative PCR and microarrays. BMC Genomics, **7**, 64.

Newman, C.G.H. (1985): Teratogen update: clinical aspects of thalidomide embryopathy-a continuing preoccupation. Teratology, **32**, 133-44.

Tanemura, K., Igarashi, K., Matsugami, T.R., Aisaki, K., Kitajima, S. and Kanno, J. (2009): Brain structure impairment and behavioral disturbance induced in male mice offspring by a single intraperitoneal administration of domoic acid (DA) to their dams. J. Toxicol. Sci., **34**, Special Issue II, SP279-SP286.